様式 C-19

科学研究費補助金研究成果報告書

平成２３年　４月１９日現在

機関番号：32622
研究種目：基盤研究（C）
研究期間：2008～2010
課題番号：20592186
研究課題名（和文）　下顎・舌・口唇・頬の協調運動を制御する神経機構の解析

研究課題名（英文）　Analysis of neural mechanisms underlying coodination of jaw, tongue, lip and cheek movements

研究代表者
井上　富雄（INOUE TOMIO）
昭和大学・歯学部・教授
研究者番号：70184760

研究成果の概要（和文）：咀嚼運動は、食物を噛み砕くだけでなく、舌や頬で食物を上下臼歯間に保持し、噛み砕いた食物が口腔外に漏出しないように口唇が閉鎖されるなど、さまざまな筋がそれぞれ正確なタイミングで動く、高度に協調した運動である。咀嚼のパターンジェネレーターは、顎口腔領域の感覚情報をもとに下顎、口唇、頬、舌の協調運動パターンを形成していると考えられるが、その詳細はほとんど明らかでない。そこで、本研究は、まず開口筋・閉口筋と表情筋との協調機構に着目し、ラットの脳幹スライス標本に膜電位感受性色素を用いた光学的電位測定法を適用し、電気刺激によって開口筋・閉口筋の運動ニューロンが存在する三叉神経運動核と表情筋の運動ニューロンが存在する顔面神経核に同時に興奮性の光学的応答を誘発する部位の検索を行った。さらに、開口筋あるいは閉口筋運動ニューロンと顔面神経運動ニューロンの同時パッチクランプ記録を行い、電気刺激あるいはレーザー光による caged グルタミン酸の解離による光刺激に対する応答を解析し、同定された部位のプレモーターニューロンからの開口筋・閉口筋運動ニューロンと表情筋運動ニューロンに対する出力様式を検討した。その結果、三叉神経運動核および顔面神経核を含む脳幹スライス標本上で、電気刺激により三叉神経運動核および顔面神経核の両方に光学的応答を誘発する領域が確認された。さらにレーザー光刺激を用いて細かく解析すると、刺激する部位により運動核に誘発される応答様式が異なった。従って、閉口筋運動ニューロンに対するプレモーターニューロンと表情筋運動ニューロンに出力を送るプレモーターニューロン群が三叉神経運動核と顔面神経核の間の網様体に存在するが、存在部位は重ならない可能性が高いことが明らかとなった。下顎運動と頬、口唇などの表情筋運動の協調運動制御は、プレモーターニューロンより上位で行われる可能性が考えられる。

研究成果の概要（英文）：Mastication is a highly coordinated movement of the jaw, tongue, lip and the cheek, in which food is hold by the tongue and cheek, and then food is crushed by the upper and lower jaws with closure of the lips. Motor commands for the coordinated movement patterns of the jaw, tongue, lip and the cheek are thought to be produced by the pattern generator for mastication; however, the detail is not still clear. In the present study, we investigated regions in frontal brainstem slice preparation from neonatal rats where premotor neurons targeting for jaw-opening, jaw-closing and facial motoneurons were located, using voltage-sensitive dye, whole-cell patch-clamp recordings and laser photostimulation in order to examine the neural mechanisms underlying coordination of the movements of jaw and facial muscles. Electrical stimulation of the reticular formation located between the trigeminal motor nucleus and the facial nucleus elicited optical responses both in the trigeminal motor nucleus and the facial nucleus. Photostimulation of the reticular formation also evoked post synaptic currents (PSCs) in jaw-opening, jaw-closing and facial motoneurons; however, the region of which photostimulation evoked PSCs in these three kinds of motoneurons were different among them. These results suggest that premotor neurons targeting for jaw-opening, jaw-closing and facial motoneurons might be differentially located in the reticular formation between the trigeminal motor nucleus and the facial nucleus.

交付決定額

（金額単位：円）

	直接経費	間接経費	合　計
2008 年度	2, 200, 000	660, 000	2, 860, 000
2009 年度	800, 000	240, 000	1, 040, 000
2010 年度	600, 000	180, 000	780, 000
年度			
年度			
総　計	3, 600, 000	1, 080, 000	4, 680, 000

研究分野：医歯薬学
科研費の分科・細目：歯学・機能系基礎歯科学
キーワード：口腔生理学、咀嚼、協調運動

１．研究開始当初の背景

1970 年代から咀嚼運動のパターン形成回路の研究がなされてきたが、本研究で明らかにしようとする、下顎、口唇・頬および舌の協調運動を司る機構についてはほとんど報告が無い。研究代表者の井上はこれまで、咀嚼力を調節する中枢神経機構の研究を一貫して行ってきた。その結果、顔面神経核背側の網様体に、口腔領域から感覚入力を受け、咀嚼リズムと同期して活動し、出力を三叉神経運動核に送るニューロンが存在することを明らかにした（Inoue et al., Nerosci Res, 1992; Inoue et al., J Neurophysiol, 1994; Takamatsu, Inoue et al., Brain Res, 2005）。この領域は、組織学的な研究から三叉・顔面・舌下神経運動核のそれぞれに出力を送る最終介在ニューロンが存在することが報告されている（Travers & Norgren, J Comp Neurol, 1983）。これらのことから顔面神経核背側の網様体は、咀嚼時の下顎、口唇・頬、舌の協調運動の制御に関与する部位の可能性がある（下図、仮説１）。

一方、Katakura ら（Jpn J Physiol, 1998）は、新生仔ラットの摘出脳幹標本に三叉神経運動核と顔面神経核との間、および顔面神経核と舌下神経核との間に横切断を加えてそれぞれの神経核の間の連絡を遮断しても、NMDA 投与による薬物刺激で三叉・顔面・舌下神経にそれぞれリズミカルな活動が誘発されることから、下顎、口唇・頬、舌の運動を制御する神経回路がそれぞれの神経核の近傍に独立して存在する可能性を示している。従って、これらの神経回路が相互連絡し、協調して活動している可能性もある（上図、仮説２）。

そこで本研究は、下顎、口唇・頬、舌の協調運動の制御機構に関してどちらの仮説が正しいか、あるいは全く別の様式の制御回路が存在するかどうかを検索するものである。

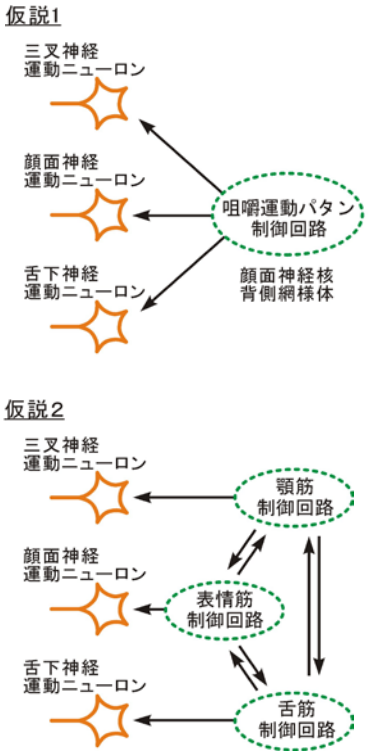

２．研究の目的

1）閉口筋運動ニューロンおよび開口筋運動ニューロンに対する premotor neuron の解析

食物を咀嚼する際の咀嚼筋活動は、食物の硬さや大きさなどの物理的な性状によってさまざまに変化する。このことは、食品の硬さについての感覚情報を受け、閉口筋および開口筋運動ニューロンに興奮性あるいは抑制性の出力を送ってその活動性を調節する premotor neuron が脳に存在することを示唆している. そこで、まずこれらの premotor neuron からの入力の特性を解析するために、新生仔ラットの水平断脳幹スライス標本に光学的電位測定法を適用し、電気刺激によって三叉神経運動核に光学的応答を誘発す

る部位をスライス標本上で検索した。これによって明らかとなった部位に電気刺激あるいは caged 化合物を使った光刺激を行い、それに対するシナプス後電流応答を咬筋運動ニューロンおよび顎二腹筋運動ニューロンから記録した。さらに発育変化についても検討を加えた。

2)三叉神経運動ニューロンおよび顔面神経運動ニューロンに興奮性出力を送る最終介在ニューロンの存在部位の検索

三叉・顔面神経運動核のいずれかを含む脳幹スライス標本を作製し、スライス標本のさまざまな部位を電気刺激した時の応答を光学的電位測定装置で観察する。運動核に興奮性の光学的応答を誘発する部位は、興奮性最終介在ニューロンを有し、該当する筋の運動制御に関わる神経回路が周囲に存在する可能性がある。脳幹をさまざまな方向に切った標本を使って、各運動核に興奮性出力を送る最終介在ニューロンの存在部位の候補を探った。これによって明らかとなった部位に電気刺激あるいは caged 化合物を使った光刺激を行い、それに対するシナプス後電流応答を咬筋運動ニューロン、顎二腹筋運動ニューロンおよび顔面神経運動ニューロンから記録し、下顎と口唇・頬の協調運動を司る神経回路についての検討を行った。

３．研究の方法

1) 閉口筋運動ニューロンおよび開口筋運動ニューロンに対する premotor neuron の解析

Wistar 系ラット(P2-11)を用いて、三叉神経運動核(MoV)を含む厚さ 500μm の水平断脳幹スライス標本を作成した。

光学的膜電位測定を行う場合は、Di-4-ANNEPS (100 μg/ml)を用いて、スライス標本を染色し、MICAM ULTIMA (Brain Vision 社)を用いて光学的応答を測定した。パッチクランプ記録を行う際は、スライス標本作成１－２日前に 3000 MW もしくは 10,000 MW の dextran-tetramethylrhodamine-lysine (RDL, 10%, 2－5 μl) を咬筋あるいは顎二腹筋に注入し、咬筋あるいは顎二腹筋運動ニューロンを逆行性に標識した。

ホールセルパッチクランプ測定には、Axopatch 200B amplifier (Molecular Devices)を用いて、RDL によって逆行性に標識された、咬筋あるいは顎二腹筋運動ニューロンから記録を行った。

また、光刺激には、窒素パルスレーザー（Micropoint, Photonic Instruments, Kawasaki, Japan, 波長 365 nm パルス幅 600 ps）装置を用い、レーザー光をガルバノレンズを介してスライス標本上の任意の点に照射し、あらかじめ灌流液中に投与した caged glutamate (4-methoxy-7-nitroindolinyl-caged L-glutamate, 300 μM, Tocris Cookson)の uncage を行った。レーザー光照射の制御ソフトウェアには、Metamorph （Molecular Devices）を用いた.

2)三叉神経運動ニューロンおよび顔面神経運動ニューロンに興奮性出力を送る最終介在ニューロンの存在部位の検索

三叉神経運動核および顔面神経核を含む矢状断スライス標本を作製し、格子状に電気刺激を行い、実験 1)と同様の方法で光学的電位測定装置を用いて、それぞれの運動核に興奮性の光学的応答を誘発する部位を検索する。

同定された部位に対して、実験 1)と同様の方法を用いて、電気刺激あるいは光刺激を行い、咬筋運動ニューロン、顎二腹筋運動ニューロンあるいは表情筋運動ニューロンの膜電流応答を記録する。

４．研究成果

実験 1)

INTRODUCTION

Premotor neurons targeting trigeminal motoneurons play an important role in oro-motor functions such as suckling, chewing, swallowing and voluntary jaw movements, by transmission of oro-motor commands to the trigeminal motoneurons that innervate the jaw-closing muscles or jaw-opening muscles. Retrograde axonal tracing studies have shown that the reticular formation dorsal to the facial nucleus (RdVII) is one of the brainstem regions containing premotor neurons that target the trigeminal motor nucleus (MoV) (Mizuno et al., 1983; Travers and Norgren, 1983; Landgren et al., 1986; Chandler et al., 1990; Li et al., 1995; Kolta et al., 2000). The RdVII receives descending inputs from the masticatory area and the primary orofacial motor area of the cerebral cortex (Yasui et al., 1985; Hatanaka et al., 2005), and RdVII premotor neurons receive orofacial sensory inputs (Takamatsu et al., 2005). The RdVII neurons also receive masticatory rhythm inputs; many of the neurons that are activated during rhythmic jaw movement can be found in the RdVII (Inoue et al., 1992; Inoue et al., 1994). Therefore, the RdVII might contribute to the control of jaw movement during oro-motor functions.

Our previous study showed that stimulus pulses to the RdVII almost always elicited masseter electromyography responses at short latencies in anesthetized rats and that microinjection of glutamate or

kainate to the RdVII evoked excitatory responses in the masseter nerve of artificially ventilated and immobilized rats (Takamatsu et al., 2005). Furthermore, a monosynaptic excitatory projection from one neuron in the RdVII to jaw-closing motoneurons was detected by spike-triggered averaging of rectified masseter nerve activity. Therefore, excitatory premotor neurons are most likely to be located in the RdVII. However, detailed properties of synaptic transmission from the RdVII to jaw-closing motoneurons; the presence or absence of inputs from the RdVII to jaw-opening motoneurons; and the postnatal development of such synaptic transmission from the RdVII to the trigeminal motoneurons are still unclear.

In the present study, we characterized synaptic inputs from the RdVII to jaw-closing and jaw-opening motoneurons in horizontal brainstem slice preparations from neonatal and juvenile rats. We demonstrate that both neonatal and juvenile jaw-closing motoneurons receive strong synaptic inputs from the RdVII through activation of glutamate, glycine and GABAA receptors, whereas input from the RdVII to jaw-opening motoneurons appears to be weak.

EXPERIMENTAL PROCEDURES

All experiments were approved by the International Animal Research Committee of Showa University in accordance with Japanese Government Law No. 105 for the care and use of laboratory animals.

Slice preparation

Experiments were performed with brainstem slices from postnatal day (P) 0-11 Wistar rats (n=82). Due to the difficulty of obtaining viable motoneurons close to the surface of the slices, we did not use rats older than P11. The day of birth was defined as P0. Animals were anesthetized deeply with ether and then decapitated. Each brain was removed rapidly and placed in cold oxygenated artificial cerebrospinal fluid (ACSF). The brainstem was cut into 500 μm horizontal sections with a microslicer (VT1000S, Leica Microsystems Japan, Tokyo, Japan). For cutting P0-7 rat brainstems, we used normal ACSF containing (in mM) 130 NaCl, 3 KCl, 2 CaCl2, 2 MgCl2, 1.25 NaH2PO4, 26 NaHCO3 and 10 glucose. For cutting P8-11 rat brainstems, we used sucrose-based modified ACSF to obtain viable motoneurons, as previously described (Nakamura et al., 2008). Modified ACSF contained (in mM) 260 sucrose, 3 KCl, 2 CaCl2, 2 MgCl2, 1.25 NaH2PO4, 26 NaHCO3 and 10 glucose. Normal ACSF and modified ACSF were aerated continuously with a 95% O2-5% CO2 gas mixture. Slices from P0-7 rats were incubated at 34° C for 1 h in normal ACSF. Slices from P8-11 rats were incubated at 34° C in a 50:50 mixture of modified and normal ACSF for 30 min and then incubated in normal ACSF for an additional 30 min. All slices were maintained at room temperature (25-27° C) in normal ACSF.

Optical recordings

Twenty slices from twenty P0-9 animals were stained in normal ACSF containing 100 μg ml-1 of fluorescent voltage-sensitive dye (Di-4-ANEPPS; Molecular Probes, Eugene, OR) for 1 h under 0.4 kgf cm-2 of 95% O2-5% CO2 gas and were subsequently rinsed in ACSF for 15 min (see Nakamura et al., 2008). Slices were transferred into a recording chamber that was mounted on an upright fluorescence microscope (BX51WI; Olympus, Tokyo, Japan), and the slices were superfused continuously with normal ACSF at a rate of 2.0 ml min-1 at room temperature with a peristaltic pump. Stimulus-evoked responses in the slice preparations were defined as the fractional change in fluorescence of the voltage-sensitive dye as measured by a CMOS camera-based optical imaging system (MiCAM Ultima, Brain Vision, Tsukuba, Japan). This system was equipped with a 510-550 nm excitation filter, a dichroic mirror, a 590 nm absorption filter (U-MWIG2, Olympus) and a 150-watt tungsten-halogen lamp (MHF-G150LR, Moritex, Tokyo, Japan) (see Nakamura et al., 2008). The CMOS camera head had a 10.0 x 10.0 mm2 imaging area (100 x 100 pixels), and a 2.5 x 2.5 mm2 area was covered by the image sensor, which was equipped with a 4x objective lens (0.28 NA, XLFluor4x/340; Olympus). Single-pulse electrical stimulation (20-30 μA, 0.2 ms pulse duration) was applied to the slices at 3 s intervals through a Teflon-insulated tungsten monopolar electrode (resistance of 400 kΩ at 500 Hz, TOG204-045, Unique Medical, Tokyo, Japan).

Fluorescence signals were measured every 1.5 s per trial, including 300 ms before stimulation, and were acquired at a rate of 3.0 ms/frame for 512 frames. The signals were averaged over 16 trials. Fluorescence changes were expressed as the percent fractional changes in the intensities of fluorescence relative to that of the reference images. The differential image, processed with a 2 x 2 (pixels in the image plane) and 2x (time frames) software filter, was represented by a pseudo-color display in which red corresponded to a fluorescence decrease and membrane depolarization. Optical data were collected and stored on a personal computer that was controlled by MiCAM Ultima-associated software (Brain Vision). To represent the time course of fluorescence change, the optical signals were inverted with an upward deflection corresponding to depolarization. The MoV was visualized through the optical imaging system as an opaque, bright oval region in the slices. The optical responses evoked in the MoV by stimulation were measured in the central region (3 x 3 pixels) of the MoV.

At the end of each experiment, the stimulation sites in the slices were marked by passing a 10 s, 20 μA negative current through the electrodes. The slices were fixed with 4% paraformaldehyde in 0.1 M phosphate buffer (PB) (pH 7.4) for at least 1 day at 4 ▪ C. The slices were then rinsed with 0.1 M phosphate buffered-saline (PBS) and incubated overnight in 5-25% sucrose/PBS at 4 ▪ C. Horizontal, 20-μm thick frozen sections were then cut with a cryostat and stained with cresyl violet. The location of the stimulation sites was confirmed by microscopic examination.

Patch-clamp recordings from jaw-closing and jaw-opening motoneurons

To distinguish jaw-closing motoneurons from jaw-opening motoneurons, we employed a fluorescence labeling technique (see Nakamura et al., 2008). Between one to two days before the slices were prepared, 62 animals were anesthetized with ether, and 2-5 μl of 10% 3,000 or 10,000 MW dextran-tetramethylrhodamine-lysine (DRL, Molecular Probes) in distilled water was injected bilaterally into the masseter or digastric muscles with a microsyringe (1010RN, Kloehn, Las Vegas, NV). After the animals recovered from the anesthesia, they were returned to their mothers while the DRL diffused. Masseter motoneurons (MMNs) or digastric motoneurons (DMNs) could be labeled one day after injection of 3,000 MW DRL solutions. When 10,000 MW DRL was used, slices could be prepared 2 days after DRL injection.

Whole-cell and gramicidin-perforated patch-clamp recordings were performed with infrared videomicroscopy (BX51WI, Olympus) using a 40x water immersion objective with differential interference contrast and epifluorescence optics. In preparations from 62 DRL-injected animals aged P1-11, the epifluorescence of the DRL-labeled MMNs and DMNs was quickly identified with the CCD camera. Patch electrodes were constructed from single-filament, 1.5 mm diameter borosilicate capillary tubing (GD-1.5, Narishige, Tokyo, Japan) with a microelectrode puller (P-97, Sutter Instruments, Novato, CA). Whole-cell recordings using the voltage-clamp configuration were carried out using an internal solution of (in mM) 103 K-gluconate, 27 KCl, 1 CaCl2, 10 HEPES, 11 EGTA, 2 MgCl2, 0.3 NaGTP, 2 NaATP and 5 lidocaine N-ethylbromide (QX314) (pH 7.3, 285-300 mOsm). Single-pulse electrical stimulation of 0.2 ms duration at intensities of 2.5-11.5 μA for MMNs (mean: 5.4 ± 0.4 μA, n=42) and 7.5-12.0 μA for DMNs (mean: 10.8 ± 0.7 μA, n=3) was applied to the slice at 2 s intervals through a Teflon-insulated tungsten monopolar electrode. In some experiments, cashew-coated stainless steel concentric bipolar stimulating electrodes (resistance of 200 kΩ at 500 Hz, outer diameter of 100 μm; USK-10, Unique Medical) were used for single-pulse electrical stimulation of 0.2 ms duration at intensities of around the threshold (1.5-7.0 μA, mean: 2.4±1.3 μA, n=4), 1.2 times (1.2T) threshold (7.5-10.0 μA, mean: 8.8 ± 0.4 μA, n=6) and 1.9T (12.5-14.0 μA, mean: 13.6 ± 0.3 μA, n=6) for evoking the postsynaptic currents (PSCs) in MMNs. To assess monosynaptic inputs from the RdVII to MMNs, we performed a minimal stimulation paradigm (Isaac et al., 1997; Gil et al., 1999) using a bipolar concentric electrode. Initial stimulus intensity was set to below the

threshold, and then the stimulus intensity was increased slowly to evoke a stable minimal response (a mixture of responses and failures, 20-60 trials, 0.2 Hz). Responses were accepted as monosynaptic if they exhibited short and constant latency that did not change with a small change of stimulus intensity. The Cl- concentration of the internal solution ([Cl-]i) was 33 mM, which was the same as that of neonatal hypoglossal motoneurons as predicted by the Nernst equation (Singer et al., 1998). Since the Cl- concentration of ACSF was 141 mM in the present study, the Cl- equilibrium potential was calculated to be -37.3 mV by the Nernst equation, which was similar to the reversal potentials of strychnine-sensitive PSCs in MMNs and DMNs of P1-4 rats using the gramicidin-perforated patch-clamp recordings in our previous study (Nakamura et al., 2008). Therefore, both the glycinergic and GABAergic currents should be inward at a holding potential of -70 mV during whole-cell recordings. Pipette resistances ranged from 2.5-5.0 MΩ when the electrodes were filled. For gramicidin-perforated patch-clamp recordings, an internal solution containing (in mM) 150 KCl, 10 HEPES (pH 7.2, 305 mOsm) was used. Gramicidin was dissolved in 10 mg ml-1 dimethyl sulfoxide and diluted in the pipette-filling solution to a final concentration of 20 μg ml-1 just immediately prior to the experiment. Stimulus-evoked PSCs in the whole-cell configuration were recorded with an Axopatch 200B amplifier (Molecular Devices, Sunnyvale, CA). Series resistance compensation was set to 70-80% for whole-cell recordings. Stimulus-evoked postsynaptic potentials (PSPs) evoked by electrical stimulation of the RdVII and membrane potentials in the gramicidin-perforated patch-clamp configuration were recorded with a Multiclamp 700B amplifier (Molecular Devices). Data were filtered at 5 kHz, digitized at 10 kHz, stored on a computer hard disk using software (pCLAMP 8.2, Molecular Devices) through an A-D converter (Digidata 1332A, Molecular Devices) and analyzed with Clampfit 8.2 (Molecular Devices) and Excel (Microsoft) software. PSC data from 4-10 trials were averaged and used for analyses. The liquid-junction potential of 11 mV was subtracted from all membrane potentials in the whole-cell patch configuration. The liquid-junction potential for gramicidin-perforated patch-clamp recordings was not corrected. All experiments were performed at room temperature.

Photostimulation

Laser photolysis of caged glutamate was performed using the Micropoint laser system (Photonic Instruments, St. Charles, IL) to stimulate RdVII neurons. A pulsed nitrogen laser (365 nm wavelength, 600 ps pulse duration; KEN-3010, USHO, Osaka, Japan) was directed into the epifluorescence ports using the beam splitters of the microscope and a pair of mirror galvanometers (Photonic Instruments), and, using a 4x 0.28 NA objective, the beam was focused onto an area of approximately 10-μm in diameter on the brain slice. Angles of the galvanometers were computer controlled with MetaMorph software (Molecular Devices), and the XY position, which was stimulated by the laser, was determined. Photostimulation was delivered to 16 different locations arranged in a 4 x 4 array with about 120 μm spacing between adjacent rows and columns, which were located caudal to the MoV and included parts of the RdVII.

After establishing the whole-cell configuration of jaw-closing motoneurons using the 40x objective with differential interference contrast and epifluorescence optics, the 40x objective was gently changed to the 4x objective. Then, 4-methoxy-7-nitroindolinil-caged L-glutamate (Tocris Cookson, Ellisville, MO) was added to 25 ml ACSF to yield a final concentration of 300 μM, and this solution was circulated. Subsequently, epifluorescence illumination was switched to photostimulation using the beam splitter. All photostimulation experiments were started at least 10 min after the addition of caged glutamate. Each pulse of photostimulation was delivered to the RdVII at 5 s intervals to trigger focal photolysis of caged glutamate. We varied the strength of photostimulation by using motorized rotary neutral density filters of varying optical densities, which were controlled

with MetaMorph software.

Drug application

For all experiments, the following drugs were applied to the bath in ACSF: 6-cyano-7-nitroquinoxaline-2,3-dione (CNQX, 20 μM, Sigma-Aldrich, St. Louis, MO), DL-2-amino-5-phosphonopentanoic acid (APV, 20 μM, Sigma-Aldrich), (±)-3(2-carboxypiperazin -4-yl)propyl-1-phosphonic acid (CPP, 10 μM, Sigma-Aldrich), strychnine (1-10 μM, Sigma-Aldrich), bicuculline (10 or 50 μM, Sigma-Aldrich), SR95531 (2 μM, Sigma-Aldrich) and tetrodotoxin (TTX, 0.5 μM, Sigma-Aldrich).

Statistics

Values are presented as mean ± S.E.M. Data obtained before, during and after drug application within groups were subjected to one-way repeated measures of analysis of variance (ANOVA). Differences in data between groups were analyzed by the Student's t test, two-way ANOVA and the $\chi 2$ test. ANOVA was followed by the Newman-Keuls post-hoc multiple comparison test when appropriate. Probability values of less than 0.05 were considered significant. Statistical analyses were conducted with SPSS 13.0J (SPSS Japan Inc.) and Microsoft Excel 2003.

RESULTS

Optical responses in the MoV evoked by electrical stimulation of the RdVII

To investigate the possibility that premotor neurons for the MoV are located in the RdVII, we examined whether the optical responses in the MoV were elicited by single-pulse electrical stimulation applied to various sites in the reticular formation caudal to the MoV. We analyzed 16 horizontal brainstem slices from 16 rats (P0-5) stained with Di-4-ANEPPS. Figure 1A left is a photograph taken during a typical experiment. The stimulating electrode was positioned caudal to the MoV. The stimulation sites in the RdVII were confirmed by histological analysis after the experiments. Stimulation of the RdVII at intensities of 20-30 μA (mean: 22.5 ± 1.2 μA) evoked optical responses in the MoV in all 16 slices examined. Activated regions 170-310 μm (mean: 237 ± 15 μm) in diameter were seen around the electrodes immediately after stimulation (Fig. 1C, 2nd frame, arrowhead). Such extent of activated areas corresponded well to the estimation of 10 μm μA-1 as an effective spread of the stimulus current through a monopolar electrode proposed by Abzug et al. (1974). The optical response in the MoV is evoked in the 3rd to 6th frames of the image series. Stimulation applied to sites outside the RdVII did not evoke optical responses in the MoV (data not shown). Excitation evoked by RdVII stimulation also propagated in the caudal direction and was stopped by the thread of the weight for slice fixation. All optical responses were completely abolished by bath application of 0.5 μM TTX (n=10, data not shown).

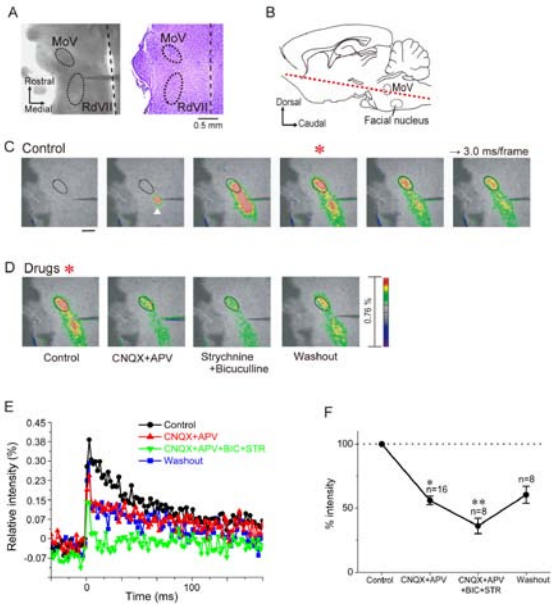

FIG. 1. Optical responses in the MoV evoked by electrical stimulation of the RdVII in a horizontal brainstem slice preparation from a P0-5 neonatal rats.

We next sought to determine which neurotransmitters are involved in synaptic transmission from the RdVII to the MoV in P0-5 rats. Using 16 slices from 16 rats, we tested the effects of several receptor antagonists of fast synaptic transmission on the optical responses in the MoV induced by RdVII stimulation. Combined bath application of the non-N-methyl-D-aspartate (non-NMDA) receptor antagonist CNQX (20 μM) and the NMDA receptor antagonist APV (20 μM) significantly reduced the peak value of optical responses in the MoV by 43.9 ± 3.3% compared to control responses (n=16,

P<0.01, one-way ANOVA; P<0.05, Newman-Keuls test; Fig. 1D, E, F). We subsequently examined the effects of addition of the glycine receptor antagonist strychnine (1-10 μM) and the GABAA receptor antagonist bicuculline (10 or 50 μM) to 8 of the 16 slices. Addition of strychnine and bicuculline further reduced the remaining optical responses by 19.9 ± 6.0% (n=8) in all 8 slices; however, the optical responses were not abolished in all 8 slices (Fig. 1D, E, F). Partial recovery of optical responses in MoV was observed after all antagonists were washed out for 40-60 min with normal ACSF (Fig. 1D, E, F). These results suggest that the RdVII likely sends glutamatergic, glycinergic and GABAergic inputs to the MoV, and that glycinergic and/or GABAergic inputs from the RdVII to the MoV are excitatory in P0-5 rats. This is similar to the excitatory glycinergic and GABAergic inputs from the supratrigeminal region (SupV) to the MoV in P1-6 rats (Nakamura et al., 2008).

RdVII stimulation-evoked postsynaptic currents in neonatal jaw-closing and jaw-opening motoneurons

To study the nature of synaptic inputs from the RdVII to trigeminal motoneurons, we used whole-cell patch-clamp recordings to examine the PSCs of trigeminal motoneurons in response to monopolar or bipolar stimulation of the RdVII. We first examined the responses of MMNs (jaw-closing motoneurons) evoked by monopolar stimulation of the RdVII in 27 slices from 26 rats aged P1-4, and the RdVII stimulation-induced inward PSCs at a holding potential of -70 mV in all 27 MMNs tested (Fig. 2). Combined application of CNQX (20 μM) and the NMDA receptor antagonist CPP (10 μM) significantly reduced the PSC amplitudes by 57.8 ± 11.1% (from 134 ± 22.1 pA in control to 60.4 ± 21.2 pA in CNQX and CPP, n=7, P<0.01) compared to control responses (Fig. 2A, D). Application of CNQX and CPP did not affect the latency of the PSCs (3.4 ± 0.5 ms in control vs. 3.7 ± 0.4 ms in CNQX and CPP, n=7, P>0.5). Partial recovery of PSCs was observed in 4 MMNs after the antagonists were washed out for 20 min with normal ACSF (Fig. 2A, D).

The aim of the next set of experiments was to identity the transmitters that were involved in the remaining PSCs that resulted from monopolar stimulation of the RdVII after application of CNQX and CPP; for these experiments, 6 MMNs (which were different from the 6 MMNs shown in Fig. 2A and 2D) were recorded in P2-4 rats. Since strychnine may reduce both GABAergic and glycinergic currents in MMNs and DMNs, we first examined the effects of the specific GABAA receptor antagonist SR95531 (2 μM), and subsequently examined the effects of addition of 10 μM strychnine. In the presence of 20 μM CNQX and 10 μM CPP, application of 2 μM SR95531 significantly decreased the CNQX- and CPP-insensitive PSC amplitudes in all 6 MMNs by 43.4 ± 5.4% (from 108 ± 32.8 pA in CNQX and CPP to 54.9 ± 14.2 pA in SR95531, n=6, P<0.01, one-way ANOVA; P<0.05, Newman-Keuls test) compared to the responses before SR95531 application (Fig. 2E). SR95531 did not affect the PSC latency (3.4 ± 0.4 ms in CNQX and CPP vs. 3.5 ± 0.3 ms in SR95531, n=6, P>0.5). Addition of 10 μM strychnine almost completely abolished the remaining PSCs in all 6 MMNs (Fig. 2E). Partial recovery of PSCs was observed in one MMN after washing out SR95531 and strychnine. The rate of decrease in the amplitudes of the CNQX- and CPP-insensitive PSCs after SR95531 application was not significantly different from the rate of decrease in the PSC amplitude after strychnine application (P>0.1).

Compared with a monopolar stimulating electrode, a more focal electrical stimulus can be delivered with a bipolar concentric electrode. Thus, we also examined the effects of SR95531 or strychnine on the CNQX- and CPP-insensitive PSCs evoked by bipolar stimulation in 6 MMNs from 6 rats aged P1-4. In the presence of 20 μM CNQX and 10 μM CPP, bipolar stimulation of the RdVII at an intensity of 1.2T induced inward PSCs, with a mean amplitude of 49.8 ± 10.6 pA at a holding potential of -70 mV, in all 6 MMNs tested. Application of 2 μM SR95531 also significantly decreased the amplitudes of CNQX- and CPP-insensitive PSC in all 6 MMNs by 48.6 ± 3.2% (n=6, P<0.01, one-way ANOVA; P<0.05, Newman-Keuls test) (Fig. 2B, E). SR95531 did not affect the PSC latency (3.4 ± 0.4 ms in CNQX and CPP vs. 3.5 ± 0.4 ms in SR95531, n=6, P>0.5). Subsequently, we

examined the effects of a low dose of strychnine (1 μM) on the remaining PSCs and found that the addition of this dose of the glycine receptor antagonist almost completely abolished the remaining PSCs in all 6 MMNs (Fig. 2B, E). Partial recovery of PSCs was observed in 2 MMNs after washing out SR95531 and strychnine. We also examined the effects of SR95531 or strychnine on the CNQX- and CPP-insensitive PSCs evoked by bipolar stimulation at higher intensities than 1.2T in the same 6 MMNs as used for 1.2T bipolar stimulation. We used a 1.9T stimulation in these experiments because stimulation at a higher intensity of 2.0T caused a bubble to form around the stimulating electrode in the slice preparations. RdVII stimulation at 1.9T evoked PSCs of 2.0T larger amplitudes (114 ± 27.9 pA, n=6) compared with those evoked by 1.2T stimulation. SR95531 significantly decreased the CNQX- and CPP-insensitive PSC amplitudes in all 6 MMNs tested by 43.6 ± 2.5% (n=6, $P<0.01$, one-way ANOVA; $P<0.05$, Newman-Keuls test) (Fig. 2E). In addition, 1 μM strychnine almost completely abolished the remaining PSCs in all 6 MMNs. Partial recovery of PSCs was observed in 2 MMNs after washing out SR95531 and strychnine. The rate of decrease in the amplitudes of the CNQX- and CPP-insensitive PSCs after SR95531 application did not significantly differ among the PSCs evoked by monopolar, 1.2T and 1.9T bipolar stimulation of the RdVII. Similarly, the rate of decrease after strychnine application did not significantly differ among the PSCs that were evoked by monopolar, 1.2T and 1.9T bipolar stimulation of the RdVII, either ($P>0.5$, two-way ANOVA) (Fig. 2E). Therefore, the fractions of GABAergic and glycinergic currents were not different among the PSCs evoked by monopolar, 1.2T and 1.9T bipolar stimulation of the RdVII.

Since we used CPP and SR95531, instead of APV and bicuculline that were used in the optical recordings, to study the nature of synaptic inputs from the RdVII to MMNs, we also examined the effects of 20 μM APV and 10 μM bicuculline on the PSCs in 4 MMNs of P2-3 rats. Application of 10 μM CNQX and 20 μM APV reduced the PSC amplitudes by 57.2 ± 8.1% (from 208.3 ± 94.1 pA in the control to 103.9 ± 62.8 pA in CNQX and APV, n=4, $P<0.05$) compared to the control responses. Subsequent addition of 10 μM bicuculline and 1 μM strychnine almost completely abolished the remaining PSCs in all 4 MMNs.

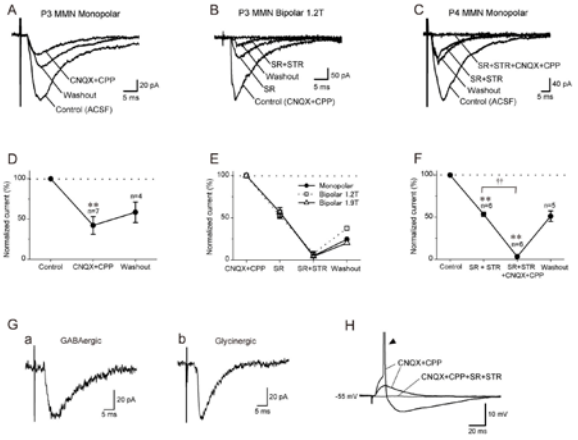

FIG. 2. Effects of receptor antagonists on the PSCs of jaw-closing motoneurons (MMNs) in P1-4 neonatal rats.

Subsequently we examined the time course of SR95531-sensitive and strychnine-sensitive PSCs. SR95531-sensitive PSCs were obtained by digital subtraction of the PSCs that were recorded in the presence of CNQX, CPP and SR95531 from the PSCs that were recorded after the application of CNQX and CPP (Fig. 2Ga). The 10-90% rise time of SR95531-sensitive PSCs was significantly longer than the rise time of strychnine-sensitive PSCs ($P<0.05$, two-way ANOVA, $P<0.05$, Newman-Keuls test) (Fig. 2G, Table 1). The 90-10% decay time of SR95531-sensitive PSCs also tended to be longer than the decay time of strychnine-sensitive PSCs; however, this difference was not significant ($P<0.05$, two-way ANOVA; $P=0.08$, Newman-Keuls test) (Table 1). The onset latencies of SR95531-sensitive and strychnine-sensitive PSCs were not significantly different ($P>0.9$, two-way ANOVA) (Table 1).

Since combined application of SR95531 and strychnine abolished CNQX- and CPP-insensitive PSCs, we next examined the nature of glutamatergic PSCs; these were pharmacologically isolated by combined application of 2 μM SR95531 and 1 μM strychnine in the absence of CNQX and CPP (6 MMNs from P1-4 rats). Using this paradigm, SR95531 and strychnine-insensitive currents should

correspond to glutamatergic currents. SR95531 and strychnine significantly reduced the PSC amplitudes that were evoked by monopolar RdVII stimulation to 53.5 ± 2.6% of the control (from 187.5 ± 21.1 pA in the control to 101.8 ± 15.3 pA in SR95531 and strychnine, n=6, $P<0.01$; Fig. 2C, F). The remaining currents were almost completely abolished in all 6 MMNs by addition of CNQX and CPP (Fig. 2C, F). The fraction of glutamatergic currents isolated by SR95531 and strychnine in the RdVII stimulation-evoked PSCs was not significantly different from the fraction of glutamatergic currents that were dissected by application of CNQX and CPP in the absence of SR95531 and strychnine ($P>0.3$, two-way ANOVA; Fig. 6I). Neither the 10-90% rise time nor the 90-10% decay time of the glutamatergic currents that were isolated by SR95531 and strychnine were significantly different from those of the glutamatergic currents that were dissected by CNQX and CPP, respectively (the rise time: $P>0.3$, two-way ANOVA; the decay time: $P>0.7$, two-way ANOVA) (Table 2).

We have previously shown in MMNs and DMNs of neonatal rats that application of GABA or glycine induces membrane depolarization and a remarkable decrease in membrane resistance and that SupV stimulation elicits an action potential (Nakamura et al., 2008). To confirm whether glycinergic or GABAergic inputs from the RdVII also excite MMNs of P1-3 neonatal rats, we performed gramicidin-perforated patch-clamp recordings of MMNs that left $[Cl^-]_i$ undisturbed (Kyrozis and Reichling, 1995) (n=4). In current clamp mode, the membrane potential was manually clamped from -55 to -60 mV by injecting a constant depolarizing current. In the presence of 20 μM CNQX and 10 μM CPP, RdVII stimulation could evoke depolarizing PSPs in all 4 MMNs tested (Fig. 2H). In 2 of the 4 MMNs an action potential was triggered by a depolarizing PSP evoked by RdVII stimulation alone (Fig. 2H, arrowhead). RdVII stimulation with simultaneous injection of a depolarizing subthreshold intracellular current pulse evoked an action potential in all 4 MMNs (see Gulledge and Stuart, 2003). Addition of 2 μM SR95531 and 1 μM strychnine completely abolished the depolarizing PSPs in all 4 MMNs. These results suggest that glycinergic or GABAergic inputs from the RdVII also excite MMNs in P1-4 rats.

To further assess monosynaptic inputs from the RdVII to MMNs, we performed a minimal stimulation paradigm (Isaac et al., 1997; Gil et al., 1999) with 4 MMNs. In the presence of 2 μM SR95531 and 1 μM strychnine, a stable minimal response (a mixture of responses and failures) was evoked in 2 MMNs at a constant latency of about 4 ms (Fig. 3Aa, c). The latency did not change with a small change in stimulus intensity, suggesting that those PSCs are presumed to originate from activation of a single presynaptic axon. Addition of 20 μM CNQX and 10 μM CPP abolished the PSCs in both MMNs tested (Fig. 3Ab, d). In two different MMNs, a stable minimal response was also evoked at a constant latency of about 4 ms in the presence of 20 μM CNQX and 10 μM CPP (Fig. 3Ba, c). Addition of 2 μM SR95531 and 1 μM strychnine abolished the PSCs in all 2 MMNs tested (Fig. 3Bb, d). These results suggest that MMNs most likely receive monosynaptic glutamatergic, and glycinergic and/or GABAergic inputs from the RdVII in P1-4 rats.

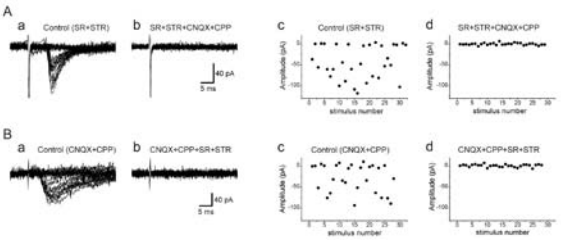

FIG. 3. Presumed monosynaptic responses in MMNs evoked by minimal stimulation of the RdVII.

We next examined whether electrical stimulation of the RdVII induced PSCs in DMNs (jaw-opening motoneurons) in 6 rats aged P3-4. Figure 4Ab shows an epifluorescence image of a representative horizontal slice and a cluster of DRL-labeled DMNs located in the mediocaudal portion of the MoV at low magnification. Cell bodies of 3 DMNs could be identified at a higher magnification (Fig. 4Ac, arrowheads). IR-DIC images of these 3 DMNs are shown in Fig. 4Ba-c, and apparent morphological differences among the 3 DMNs could not be found. We performed patch-clamp

recordings from each of the 3 DMNs, and only one DMN, indicated by the arrowhead in Fig. 4Bb, responded to monopolar stimulation of the RdVII. We examined the effects of RdVII stimulation at intensities larger than 30 μA on a total of 16 DMNs. However, PSCs were evoked in only 3 DMNs, with latencies of 4.0 ± 0.3 ms. In these 3 DMNs, PSCs could be induced by stimulation ranging from 7.5-12.0 μA. On the other hand, PSCs were evoked in all 57 MMNs tested by RdVII stimulation. The rate of occurrence of RdVII stimulation-evoked PSCs in DMNs was significantly lower than that observed in MMNs ($\chi 2$ test, $P<0.01$). The time course and the latencies of the PSCs in DMNs were not different from those in P1-4 MMNs. We did not perform further analysis of DMNs because of the low probability of encountering DMNs that responded to RdVII stimulation.

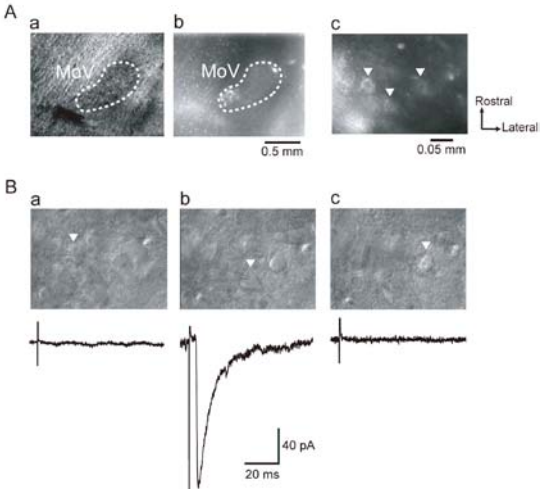

FIG. 4. Responses in jaw-opening motoneurons (DMNs) to monopolar RdVII stimulation.

Responses of MMNs to photostimulation of the RdVII

Since electrical stimulation may have activated axons of passage in the RdVII, the optical responses in the MoV and the PSCs in MMNs may have been due to activation of neurons located in areas other than the RdVII. To ascertain whether premotor neurons projecting onto MMNs are located in the RdVII, we examined whether selective activation of RdVII neurons with photolysis of caged glutamate induced PSCs in the MMNs of P3-4 rats (n=5). Whole-cell patch-clamp recordings were obtained from 5 MMNs from 5 slices. The intensity of the laser was adjusted so that, when focused on the MMNs, it would be slightly stronger than the threshold for generating an action potential in the recorded MMNs (data not shown). As shown in Fig. 5A, we delivered photostimulation to 16 locations arranged in a 4 x 4 array including parts of the RdVII. The representative responses of an MMN to photostimulation were superimposed on a photomicrograph. The largest responses, which consisted of a burst of rapidly rising inward currents, were evoked at a latency of 10 ms when the position indicated by "c" in Fig. 5A was stimulated (Fig. 5Bc). The mean latency of the largest current response in each MMN was 8.5 ± 2.5 ms (6.4-12.6 ms; n=5). When the recorded MMN indicated by "a" in Fig. 5A was stimulated, slowly rising currents, which were most likely evoked by direct stimulation of the recorded MMN by uncaged glutamate, were observed at a much shorter latency of 1.2 ms (Fig. 5Ba). These results suggest that the premotor neurons targeting MMNs are located in the RdVII.

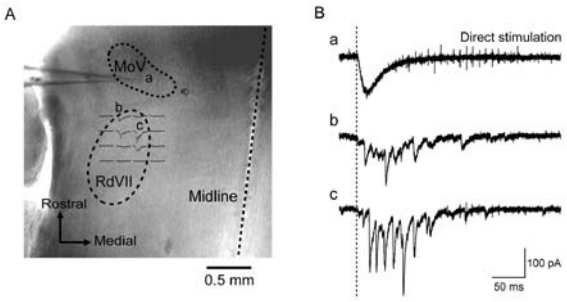

FIG. 5. Laser photolysis of caged glutamate in the RdVII. (A) Video image of a horizontal slice preparation from a P2 rat overlaid with current responses from a P3 MMN evoked by photostimulation at each location.

RdVII stimulation-evoked optical responses in the MoV and postsynaptic currents of MMNs in P8-11 rats

Our previous studies show that GABAergic and glycinergic synaptic inputs to trigeminal motoneurons in rats change from excitatory to inhibitory at approximately 7 days of age (Nakamura et al., 2008). We have also shown that the input resistance, the incidence of post-spike after depolarization, and the amplitude and half-duration of the medium-duration after hyperpolarization of MMNs change during postnatal development in rats (Yamaoka et al., 2005). Thus,

glutamatergic, GABAergic and glycinergic currents in the RdVII stimulation-evoked PSCs of MMNs might change during postnatal development. Therefore, we examined the effects of CNQX and CPP, strychnine and SR95531 on RdVII stimulation-evoked optical responses in the MoV and PSCs of MMNs in P8-11 rats. We then compared these effects of the antagonists on the PSCs between P1-4 and P8-11 rats.

In P9 rats, monopolar electrical stimulation of the RdVII at intensities of 20-30 μA also evoked the optical responses in the MoV in all 4 slices examined. In contrast to P0-5 rats, combined bath application of 10 μM bicuculline and 1 μM strychnine significantly enhanced the peak value of optical responses in the MoV by 33.0 ± 10.7% compared to control responses (n=4, $P<0.01$, one-way ANOVA; $P<0.05$, Newman-Keuls test; Fig. 6A, B). Addition of CNQX (20 μM) and APV (20 μM) reduced the optical responses in the MoV in all 4 slices examined by 75.6 ± 6.4% compared with control responses (n=4; Fig. 6A, B). The remaining optical responses were completely abolished by bath application of 0.5 μM TTX (n=4, Fig. 6A, B). Partial recovery of optical responses in the MoV was observed after all antagonists and TTX were washed out for 60 min with normal ACSF (Fig. 6A, B). These results suggest that the RdVII likely sends glutamatergic, glycinergic and GABAergic inputs to the MoV in P8-11 rats; however, glycinergic and/or GABAergic inputs from the RdVII to the MoV are most likely inhibitory.

Monopolar RdVII stimulation also evoked PSCs in all 11 MMNs tested (Fig. 6C, D, F, G). Combined application of 20 μM CNQX and 10 μM CPP significantly decreased the PSC amplitudes by 69.5 ± 5.9% in all 6 MMNs tested (from 220 ± 33.5 pA in control to 70.5 ± 17.5 pA in CNQX and CPP, $P<0.01$ Fig. 6C, F). Partial recovery of PSCs was observed in 5 MMNs after the antagonists were washed out for 20 min with normal ACSF. We also isolated glutamatergic PSCs with SR95531 and strychnine, as performed in P1-4 MMNs. Combined application of 2 μM SR95531 and 1 μM strychnine significantly reduced the amplitudes of PSCs evoked by monopolar RdVII stimulation to 57.8 ± 4.9% of the control (from 112 ± 14.1 pA in the control to 63.9 ± 8.6 pA in SR95531 and strychnine, n=5, $P<0.05$; Fig. 6D, G). The remaining currents were almost completely abolished by addition of CNQX and CPP in all 5 MMNs (Fig. 6D, G). The fraction of glutamatergic currents isolated by SR95531 and strychnine in the RdVII stimulation-evoked PSCs was not significantly different from the fraction of glutamatergic currents dissected by CNQX and CPP in the absence of SR95531 and strychnine ($P>0.3$, two-way ANOVA; Fig. 6I). Neither the 10-90% rise time nor the 90-10% decay time of the glutamatergic currents isolated by SR95531 and strychnine was significantly different from those of the glutamatergic currents dissected by CNQX and CPP, respectively (the rise time, $P>0.3$, two-way ANOVA; the decay time, $P>0.9$; two-way ANOVA) (Table 2). Neither fractions of glutamatergic currents isolated by SR95531 and strychnine, nor those dissected by CNQX and CPP in the RdVII stimulation-evoked PSCs of P8-11 rats were different from the fractions of glutamatergic currents that were isolated by SR95531 and strychnine nor those that were dissected by CNQX and CPP in P1-4 rats, respectively ($P>0.3$, two-way ANOVA; Fig. 6I).

The effects of strychnine and SR95531 on the remaining PSCs after application of CNQX and CPP were examined in eight P8-11 MMNs, which were different from the 11 MMNs shown in Fig. 6F and 6G. In the presence of 20 μM CNQX and 10 μM CPP, 2 μM SR95531 significantly decreased the amplitudes of the CNQX- and CPP-insensitive PSCs by 57.8 ± 8.9% in all 8 MMNs tested ($P<0.01$, one-way ANOVA; $P<0.01$, Newman-Keuls test; Fig. 6E, H). Addition of 10 μM strychnine almost completely abolished the remaining PSCs in all 8 MMNs (Fig. 6 E, H). The SR95531-sensitive component of the amplitudes of the CNQX and CPP-insensitive PSCs was not significantly different from the strychnine-sensitive component of the PSCs of P8-11 rats ($P>0.3$; Fig. 6J). The SR95531-sensitive component of the PSC amplitudes of P8-11 rats was not different from the SR95531-sensitive component in P2-4 rats, and the strychnine-sensitive current component of the PSC amplitudes of P8-11 rats was not different from the strychnine-sensitive component of P2-4 rats, either ($P>0.8$, two-way ANOVA; Fig. 6J). Partial recovery of PSCs was observed in 3 MMNs after washing out the

antagonists. These results suggest that the fractions of glutamatergic, GABAergic and glycinergic currents in the RdVII stimulation-evoked PSCs of MMNs do not appear to change during postnatal development from P1 to P11.

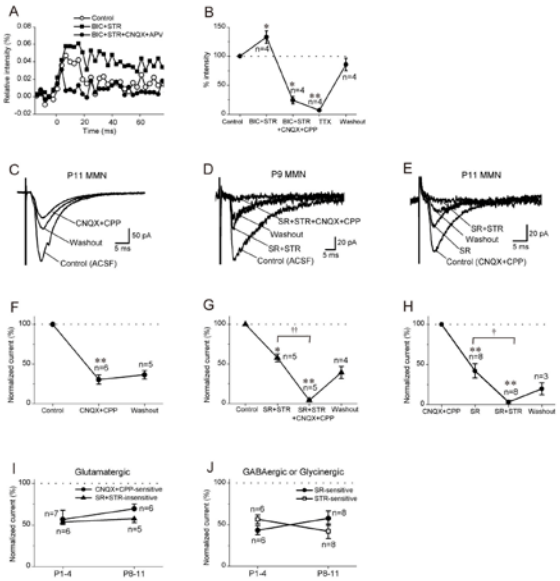

FIG. 6. Optical responses in the MoV and PSCs in MMNs evoked by monopolar RdVII stimulation in P8-11 rats.

We also examined the time course of SR95531-sensitive and strychnine-sensitive PSCs in P8-11 rats. The 10-90% rise time and the 90-10% decay time of SR95531-sensitive PSCs tended to be longer than those of strychnine-sensitive PSCs, respectively; however, these differences were not significant (10-90% rise time, $P<0.05$, two-way ANOVA, $P=0.12$, Newman-Keuls test; 90-10% decay time, $P<0.05$, two-way ANOVA, $P=0.17$, Newman-Keuls test) (Table 1). On the other hand, the 10-90% rise times of both SR95531-sensitive and strychnine-sensitive PSCs of P8-11 rats were significantly shorter than those of P2-4 rats, respectively ($P<0.01$, two-way ANOVA; SR95531-sensitive, $P<0.01$, Newman-Keuls test; strychnine-sensitive, $P<0.01$, Newman-Keuls test) (Table 1). The 90-10% decay time of SR95531-sensitive PSCs was also significantly shorter in P8-11 rats than in P2-4 rats ($P<0.05$, two-way ANOVA; SR95531-sensitive, $P<0.05$, Newman-Keuls test), and the 90-10% decay time of strychnine-sensitive PSCs tended to be shorter in P8-11 rats than in P2-4 rats, although the latter difference was not significant ($P=0.08$, Newman-Keuls test) (Table 1). The onset latencies of the PSCs were not significantly different between SR95531-sensitive and strychnine-sensitive PSCs ($P>0.7$, two-way ANOVA) (Table 1). There was also no significant difference in the onset latencies of the PSCs of each age group ($P>0.2$, two-way ANOVA) (Table 1).

DISCUSSION

Optical responses in the MoV evoked by the RdVII

In both P0-5 and P9 rats, electrical stimulation of the RdVII evoked optical responses in the MoV, which were greatly reduced by simultaneous application of glutamate, glycine and GABAA receptor antagonists; however, the optical responses were not entirely abolished. Since combined application of the same or lower doses of the antagonists that were used to test their effects on the optical responses, abolished the PSCs of MMNs evoked by RdVII stimulation in whole-cell patch-clamp recordings, the presence of the remaining optical responses did not appear to be due to ineffectiveness of the antagonists. However, TTX completely abolished all optical responses. These results suggest that neuronal excitation, which was not mediated by synaptic transmission, is likely to be involved in the optical responses in the MoV. Since we used thick (500 μm) horizontal slice preparations, interneurons sending their axons into the RdVII might be located dorsally or ventrally to the cluster of trigeminal motoneurons. It has also been reported that interneurons are located within the MoV (Mizuno et al., 1983; Travers and Norgren, 1983; McDavid et al., 2006). Therefore, the interneurons that send their axons into the RdVII might be antidromically activated by RdVII stimulation. Furthermore, the accessory trigeminal motor nucleus is located caudal to the MoV (Szekely and Matesz, 1982). The axons of motoneurons in the accessory trigeminal motor nucleus run in the rostral and dorsal direction to the MoV, and join the trigeminal motor root with a lateral and ventral bend. The caudal part of this nucleus might be located in the activated region between the RdVII and the MoV (Fig. 1C), and some motoneurons in this nucleus might be directly activated by

RdVII stimulation. Such activation could also contribute to the optical responses that are observed in the MoV region when the RdVII is stimulated.

Glutamatergic inputs to MMNs from the RdVII

Electrical stimulation of the RdVII evoked optical responses in the MoV and as well as PSCs in MMNs, and application of CNQX and APV or CPP reduced the optical responses and the PSCs by 44% and 58% in P0-5 rats, respectively. The latency of the PSCs in MMNs evoked by monopolar RdVII stimulation was around 3.4 ms, similar to the latency (3.0 ± 0.1 ms) of antidromic activation of the supratrigeminal premotor neurons located dorsal to the MoV in P1-5 rats by MoV stimulation (Nakamura et al., 2008). Furthermore, a stable glutamatergic minimal response was evoked in 2 MMNs by RdVII stimulation at just above the threshold. Thus, the PSCs in MMNs were most likely to be evoked monosynaptically by RdVII stimulation. We used low intensities of currents for monopolar stimulation (2.5-11.5 μA, mean: 4.8 ± 0.4 μA) to evoke glutamatergic PSCs in the MMNs. According to the estimation of 10 μm μA-1 as an effective spread of the stimulus current through a monopolar electrode, as proposed by Abzug et al. (1974), activated areas are likely to be confined to an area less than 120 μm diameter in the RdVII. Furthermore, the regions in which photostimulation evoked the largest PSCs in MMNs were found in the RdVII. Therefore, a certain number of glutamatergic excitatory premotor neurons targeting the MMNs are most likely located in the RdVII.

Premotor neurons, which were retrogradely labeled by tracer injection into the MoV, were located in many areas in the brainstem, including the parabrachial, supratrigeminal, and intertrigeminal regions; the lateral region of the rostral part of the medullary reticular formation; the dorsal and lateral parts of the caudal portion of the medullary reticular formation; and the dorsal parts of the principal sensory, oral spinal, and interpolar spinal trigeminal nuclei (Mizuno et al., 1983; Travers and Norgren, 1983; Landgren et al., 1986; Chandler et al., 1990; Li et al., 1995; Kolta et al., 2000). Premotor neurons responding to antidromic stimulation of the MoV have also been found in these regions (Donga and Lund, 1991; Inoue et al., 1992; Inoue et al., 1994; Westberg et al., 1995). Immunohistochemical studies have shown that not only glutamatergic premotor neurons but also GABAergic and glycinergic premotor neurons are found in these regions in guinea pigs (Turman and Chandler, 1994a; Turman and Chandler, 1994b), rabbits (Kolta et al., 2000) and rats (Li et al., 1996; Travers et al., 2005; Pang et al., 2009). Our previous study showed that electrical stimulation of, or microinjection of glutamate or kainite into, the RdVII evoked excitatory masseter responses, whereas regions other than the RdVII, the SupV and the adjacent areas did not evoke excitatory masseter responses (Takamatsu et al., 2005). Furthermore, the RdVII was the only site to elicit excitatory optical responses in the MoV of horizontal brainstem slices in the present study.

There are two possible explanations for these findings. First, premotor neurons sending relatively strong excitatory inputs to MMNs might be located in the RdVII. In fact, we found one such excitatory premotor neuron in the RdVII of an anesthetized rat, i.e., averaging of rectified masseter nerve activity after the spike potentials of this neuron revealed a monosynaptic excitatory response in nerve activity (Takamatsu et al., 2005). Second, excitatory premotor neurons targeting the MoV might be abundant in the RdVII compared with inhibitory premotor neurons, because the number of glutamatergic premotor neurons (those expressing vesicular glutamate transporter VGLUT2) in the RdVII is more than twice the number of GABAergic premotor neurons in rats (Travers et al., 2005).

Glycinergic and GABAergic inputs from the RdVII to MMNs

Electrophysiological studies have shown that switching from GABAergic to glycinergic transmission in inhibitory synapses may occur during postnatal development in the brainstem auditory system (Kotak et al., 1998; Turecek and Trussell, 2002; Nabekura et al., 2004),

the dorsal horn (Keller et al., 2001), and spinal (Gao et al., 2001) and hypoglossal (Muller et al., 2006) motoneurons. In the present study, the fraction of GABAergic currents in the RdVII stimulation-evoked PSCs of MMNs was not different from the fraction of glycinergic currents in both P2-4 and P8-11 rats; this suggest that Cl--mediated PSCs from RdVII to MMNs were likely to be equally glycinergic and GABAergic in both age groups, although glycinergic miniature IPSCs have predominantly been recorded from hypoglossal motoneurons in P0-5 rats (Donato and Nistri, 2000) and from spinal motoneurons in P1-3 rats (Gao et al., 2001). There have been reports of profound switching from GABAergic to glycinergic transmission has been reported to be profound after P11 in the developing auditory system (Kotak et al., 1998; Turecek and Trussell, 2002; Nabekura et al., 2004). In hypoglossal motoneurons, neither amplitudes of glycinergic unitary IPSCs nor GABAergic miniature IPSCs were significantly different between P0-3 and P10-18 rats, and between P1-3 and P9-13 rats, respectively (Singer et al., 1998; Sebe et al., 2003), although ethanol has been shown to differentially affect the GABAergic and glycinergic PSCs (Sebe et al., 2003). Furthermore, an immunohistochemical study showed that the fraction of boutons that synapsed onto MMNs and were immunoreactive only to GABA was similar to the fraction of boutons immunoreactive only to glycine in P2 and P11 rats, whereas the fraction of boutons immunoreactive only to GABA decreased while the fraction of boutons immunoreactive only to glycine increased in P31 rats (Paik et al., 2007). Thus the switching from GABAergic to glycinergic transmission is likely to occur in MMNs of rats older than P11. Rats start immature chewing at around P12 (Westneat and Hall, 1992), and quick inhibition of jaw-closing muscle activities is most likely necessary to prevent the oral mucosa from bites. Since glycinergic IPSCs have a faster rise time compared with GABAergic IPSCs in MMNs, glycinergic inhibition likely becomes more important in rats older than P11.

As described above, Cl^--mediated PSCs from RdVII to MMNs were likely to be equally glycinergic and GABAergic in both P2-4 and P8-11 rats. However, these results do not necessarily indicate that glycinergic premotor neurons and GABAergic premotor neurons are present in equal numbers in the RdVII of both age groups for the following reasons. First, glycine and GABA can be co-released from the same presynaptic vesicle (Jonas et al., 1998), and different kinds of vesicles that store and release one or more transmitters exist in individual boutons (Nabekura et al., 2004). Second, the numbers of postsynaptic glycine or GABA receptors may be unrelated to the numbers of presynaptic glycine or GABA terminals (Muller et al., 2006), and presynaptic elements of the inhibitory synapses in the hypoglossal nuclei of mice can follow different developmental patterns from the postsynaptic elements (Muller et al., 2006; Muller et al., 2008). Third, technical restrictions that influence the ability to record precise PSCs may affect the results obtained in the present study. In large neurons such as MMNs, voltage-clamp of the soma to -70 mV may not guarantee clamping the tip of the dendrite, and the spatial constraints of dialyzing the cell with the pipette solution might cause nonuniform driving forces between inhibitory synapses located in the soma and those in the dendrites. Therefore, glycinergic and/or GABAergic postsynaptic events that occurred in synapses on the distal dendrites might be recorded with an inaccurately small amplitude. Further studies are needed to clarify the properties of glycinergic and/or GABAergic premotor neurons targeting MMNs.

Unlike the inputs from the RdVII, MMNs receive weaker GABAergic inputs from the SupV as compared with glycinergic inputs, even in rats as young as P1-4 (Nakamura et al 2008). The SupV is assumed to contain glycinergic premotor neurons that inhibit jaw-closing motoneurons during the jaw-opening reflex (Goldberg and Nakamura, 1968; Kidokoro et al., 1968; Nakamura et al., 1973). Such glycinergic premotor neurons are likely to exist even at birth, and GABAergic premotor neurons may become already minor in the SupV at birth.

Inputs to DMNs from the RdVII

Compared with the responses of MMNs to electrical stimulation of the RdVII, only three neurons out of the 16 DMNs tested

responded to RdVII stimulation. There are two possible explanations for the rarity of this DMN response. First, quite a few premotor neurons targeting the DMNs may be located in the RdVII. Two studies have shown histologically that the pattern of distribution of retrogradely labeled premotor neurons after injection of a retrograde tracer into the dorsolateral division of the MoV, where jaw-closing motoneurons are located, is different from the pattern in the ventromedial division of the MoV, where jaw-opening motoneurons are located (Li et al., 1995; Yamamoto et al., 2007), although the patterns of distribution of the premotor neurons are slightly different between these two studies. Furthermore, Yoshida et al. (2001) examined the synaptic contacts made between the neurons in the rostrodorsomedial part of the oral spinal trigeminal nucleus and the trigeminal motoneurons by using the intracellular staining method. They showed that the premotor neurons targeting MMNs are located more laterally or dorsally in the oral spinal trigeminal nucleus compared with the premotor neurons targeting DMNs. Thus, it is possible that many premotor neurons targeting MMNs are located in the RdVII whereas premotor neurons targeting DMNs are sparse in this region. A second possibility is that premotor neurons targeting DMNs in the RdVII may send their axons in a dorsal or ventral direction, beyond the superior or inferior surfaces of the slice preparations. After injection of a retrograde tracer into the ventromedial division of the MoV, many labeled premotor neurons were found in the RdVII (Li et al., 1995; Yamamoto et al., 2007). However, Bourque and Kolta (2001) have suggested that interneurons in the surrounding area of the MoV, including the parvocellular reticular formation caudal to the MoV, send their axons into the areas surrounding the MoV. Thus, if leakage of the retrograde tracers from the MoV to the surrounding area occurs, the tracers could be taken up into the terminal of axons whose cell bodies are located in the RdVII. The dye would then be transported to the cell bodies in the RdVII. Further studies are necessary to confirm whether premotor neurons targeting DMNs are located in the RdVII.

Functional roles of premotor neurons in the RdVII

Application of high-frequency, short-train electrical stimulation to the primary orofacial motor areas of the cerebral cortex induces twitch-like jaw movements accompanied by activation of jaw-opening and jaw-closing muscles in monkeys (Clark and Luschei, 1974; Hatanaka et al., 2005). Repetitive electrical stimulation of the cortical masticatory area induces rhythmic jaw and tongue movements similar to the movements that occur during mastication in many species, including rats (Sasamoto et al., 1990; Zhang and Sasamoto, 1990) and monkeys (Walker and Green, 1938; Lund and Lamarre, 1974; Hatanaka et al., 2005). However, activation of neurons in these cortical areas must be transmitted to the MoV by way of premotor neurons in the brainstem because these cortical areas send very few, if any, projection fibers directly to the MoV (Zhang and Sasamoto, 1990; Enomoto et al., 1995; Hatanaka et al., 2005). The RdVII has been shown to receive dense inputs from both the primary orofacial motor cortex and cortical masticatory area (Yasui et al., 1985; Hatanaka et al., 2005; Yoshida et al., 2009). Therefore, motor commands from these cortical areas might be conveyed by way of RdVII premotor neurons. Furthermore, many rhythmically active neurons can be found in the RdVII of anesthetized and immobilized rats (Inoue et al., 1992) and guinea pigs (Inoue et al., 1994) during cortically-induced rhythmic jaw movement. Thus, it is possible that stimulation of the cortical masticatory area activates RdVII neurons and/or RdVII premotor neurons, leading to rhythm generation of suckling and/or mastication in the RdVII. If this is the case, the suckling and/or masticatory rhythms generated in the RdVII may be transmitted to the MoV by RdVII premotor neurons.

Optical responses evoked by RdVII stimulation were propagated in the caudal direction from the RdVII, as well as into the MoV, suggesting that inputs from the RdVII are conveyed to some areas caudal to the RdVII. Travers et al. (2005) have shown that a number of premotor neurons target the MoV or the hypoglossal nucleus in the RdVII, and that the RdVII contains premotor neurons projecting to both the

MoV and the hypoglossal nucleus. If RdVII premotor neurons directly or indirectly send their axons to hypoglossal and trigeminal motoneurons, they could contribute to the coordination of jaw and tongue movement during mastication and/or suckling. Thus, RdVII premotor neurons may be important in the control of suckling, mastication and/or voluntary jaw movements.

Acknowledgements

This work was supported in part by MEXT.HAITEKU (2005-2009); a Showa University grant-in-aid for innovative collaborative research projects; a special research grant-in-aid for development of characteristic education; and MEXT grants-in-aid for scientific research (nos. 18890191 and 20592186).

REFERENCES

Abzug C, Maeda M, Peterson BW, Wilson VJ (1974) Cervical branching of lumbar vestibulospinal axons. J Physiol 243:499-522.

Bourque MJ, Kolta A (2001) Properties and interconnections of trigeminal interneurons of the lateral pontine reticular formation in the rat. J Neurophysiol 86:2583-2596.

Chandler SH, Turman J, Jr., Salem L, Goldberg LJ (1990) The effects of nanoliter ejections of lidocaine into the pontomedullary reticular formation on cortically induced rhythmical jaw movements in the guinea pig. Brain Res 526:54-64.

Clark RW, Luschei ES (1974) Short latency jaw movement produced by low intensity intracortical microstimulation of the precentral face area in monkeys. Brain Res 70:144-147.

Donato R, Nistri A (2000) Relative contribution by GABA or glycine to Cl(-)-mediated synaptic transmission on rat hypoglossal motoneurons in vitro. J Neurophysiol 84:2715-2724.

Donga R, Lund JP (1991) Discharge patterns of trigeminal commissural last-order interneurons during fictive mastication in the rabbit. J Neurophysiol 66:1564-1578.

Enomoto S, Kohase H, Nakamura Y (1995) Dual brain stem projection from the cortical masticatory area in guinea-pig. Neuroreport 6:1573-1577.

Gao BX, Stricker C, Ziskind-Conhaim L (2001) Transition from GABAergic to glycinergic synaptic transmission in newly formed spinal networks. J Neurophysiol 86:492-502.

Gil Z, Connors BW, Amitai Y (1999) Efficacy of thalamocortical and intracortical synaptic connections: quanta, innervation, and reliability. Neuron 23:385-397.

Goldberg LJ, Nakamura Y (1968) Lingually induced inhibition of masseteric motoneurones. Experientia 24:371-373.

Gulledge AT, Stuart GJ (2003) Excitatory actions of GABA in the cortex. Neuron 37:299-309.

Hatanaka N, Tokuno H, Nambu A, Inoue T, Takada M (2005) Input-output organization of jaw movement-related areas in monkey frontal cortex. J Comp Neurol 492:401-425.

Inoue T, Chandler SH, Goldberg LJ (1994) Neuropharmacological mechanisms underlying rhythmical discharge in trigeminal interneurons during fictive mastication. J Neurophysiol 71:2061-2073.

Inoue T, Masuda Y, Nagashima T, Yoshikawa K, Morimoto T (1992) Properties of rhythmically active reticular neurons around the trigeminal motor nucleus during fictive mastication in the rat. Neurosci Res 14:275-294.

Isaac JT, Crair MC, Nicoll RA, Malenka RC (1997) Silent synapses during development of thalamocortical inputs. Neuron 18:269-280.

Jonas P, Bischofberger J, Sandkuhler J (1998) Corelease of two fast neurotransmitters at a central synapse. Science 281:419-424.

Keller AF, Coull JA, Chery N, Poisbeau P, De Koninck Y (2001) Region-specific developmental specialization of GABA-glycine cosynapses in laminas I-II of the rat spinal dorsal horn. J Neurosci 21:7871-7880.

Kidokoro Y, Kubota K, Shuto S, Sumino R (1968) Reflex organization of cat masticatory muscles. J Neurophysiol 31:695-708.

Kolta A, Westberg KG, Lund JP (2000) Identification of brainstem interneurons projecting to the trigeminal motor nucleus and adjacent structures in the rabbit. J Chem Neuroanat 19:175-195.

Kotak VC, Korada S, Schwartz IR, Sanes DH (1998) A developmental shift from GABAergic to glycinergic transmission in the central auditory system. J Neurosci 18:4646-4655.
Kyrozis A, Reichling DB (1995) Perforated-patch recording with gramicidin avoids artifactual changes in intracellular chloride concentration. J Neurosci Methods 57:27-35.
Landgren S, Olsson KA, Westberg KG (1986) Bulbar neurones with axonal projections to the trigeminal motor nucleus in the cat. Exp Brain Res 65:98-111.
Li YQ, Takada M, Kaneko T, Mizuno N (1995) Premotor neurons for trigeminal motor nucleus neurons innervating the jaw-closing and jaw-opening muscles: differential distribution in the lower brainstem of the rat. J Comp Neurol 356:563-579.
Li YQ, Takada M, Kaneko T, Mizuno N (1996) GABAergic and glycinergic neurons projecting to the trigeminal motor nucleus: a double labeling study in the rat. J Comp Neurol 373:498-510.
Lund JP, Lamarre Y (1974) Activity of neurons in the lower precentral cortex during voluntary and rhythmical jaw movements in the monkey. Exp Brain Res 19:282-299.
McDavid S, Lund JP, Auclair F, Kolta A (2006) Morphological and immunohistochemical characterization of interneurons within the rat trigeminal motor nucleus. Neuroscience 139:1049-1059.
Mizuno N, Yasui Y, Nomura S, Itoh K, Konishi A, Takada M, Kudo M (1983) A light and electron microscopic study of premotor neurons for the trigeminal motor nucleus. J Comp Neurol 215:290-298.
Muller E, Le Corronc H, Scain AL, Triller A, Legendre P (2008) Despite GABAergic neurotransmission, GABAergic innervation does not compensate for the defect in glycine receptor postsynaptic aggregation in spastic mice. Eur J Neurosci 27:2529-2541.
Muller E, Le Corronc H, Triller A, Legendre P (2006) Developmental dissociation of presynaptic inhibitory neurotransmitter and postsynaptic receptor clustering in the hypoglossal nucleus. Mol Cell Neurosci 32:254-273.
Nabekura J, Katsurabayashi S, Kakazu Y, Shibata S, Matsubara A, Jinno S, Mizoguchi Y, Sasaki A, Ishibashi H (2004) Developmental switch from GABA to glycine release in single central synaptic terminals. Nat Neurosci 7:17-23.
Nakamura S, Inoue T, Nakajima K, Moritani M, Nakayama K, Tokita K, Yoshida A, Maki K (2008) Synaptic transmission from the supratrigeminal region to jaw-closing and jaw-opening motoneurons in developing rats. J Neurophysiol 100:1885-1896.
Nakamura Y, Mori S, Nagashima H (1973) Origin and central pathways of crossed inhibitory effects of afferents from the masseteric muscle on the masseteric motoneuron of the cat. Brain Res 57:29-42.
Paik SK, Bae JY, Park SE, Moritani M, Yoshida A, Yeo EJ, Choi KS, Ahn DK, Moon C, Shigenaga Y, Bae YC (2007) Developmental changes in distribution of gamma-aminobutyric acid- and glycine-immunoreactive boutons on rat trigeminal motoneurons. I. Jaw-closing motoneurons. J Comp Neurol 503:779-789.
Pang YW, Ge SN, Nakamura KC, Li JL, Xiong KH, Kaneko T, Mizuno N (2009) Axon terminals expressing vesicular glutamate transporter VGLUT1 or VGLUT2 within the trigeminal motor nucleus of the rat: origins and distribution patterns. J Comp Neurol 512:595-612.
Sasamoto K, Zhang G, Iwasaki M (1990) Two types of rhythmical jaw movements evoked by stimulation of the rat cortex. Shika Kiso Igakkai Zasshi 32:57-68.
Sebe JY, Eggers ED, Berger AJ (2003) Differential effects of ethanol on GABA(A) and glycine receptor-mediated synaptic currents in brain stem motoneurons. J Neurophysiol 90:870-875.
Singer JH, Talley EM, Bayliss DA, Berger AJ (1998) Development of glycinergic synaptic transmission to rat brain stem motoneurons. J Neurophysiol 80:2608-2620.
Szekely G, Matesz C (1982) The accessory motor nuclei of the trigeminal, facial, and abducens nerves in the rat. J Comp Neurol 210:258-264.
Takamatsu J, Inoue T, Tsuruoka M, Suganuma T, Furuya R, Kawawa T (2005) Involvement of reticular neurons located dorsal to the facial nucleus in activation of the jaw-closing muscle in rats. Brain Res

1055:93-102.
Travers JB, Norgren R (1983) Afferent projections to the oral motor nuclei in the rat. J Comp Neurol 220:280-298.
Travers JB, Yoo JE, Chandran R, Herman K, Travers SP (2005) Neurotransmitter phenotypes of intermediate zone reticular formation projections to the motor trigeminal and hypoglossal nuclei in the rat. J Comp Neurol 488:28-47.
Turecek R, Trussell LO (2002) Reciprocal developmental regulation of presynaptic ionotropic receptors. Proc Natl Acad Sci U S A 99:13884-13889.
Turman J, Jr., Chandler SH (1994a) Immunohistochemical evidence for GABA and glycine-containing trigeminal premotoneurons in the guinea pig. Synapse 18:7-20.
Turman JE, Jr., Chandler SH (1994b) Immunohistochemical localization of glutamate and glutaminase in guinea pig trigeminal premotoneurons. Brain Res 634:49-61.
Walker, Green (1938) Electrical excitability of the motor face area: a comparative study in primates. J Neurophysiol 152-165.
Westberg KG, Sandstrom G, Olsson KA (1995) Integration in trigeminal premotor interneurones in the cat. 3. Input characteristics and synaptic actions of neurones in subnucleus-gamma of the oral nucleus of the spinal trigeminal tract with a projection to the masseteric motoneurone subnucleus. Exp Brain Res 104:449-461.
Westneat MW, Hall WG (1992) Ontogeny of feeding motor patterns in infant rats: an electromyographic analysis of suckling and chewing. Behav Neurosci 106:539-554.
Yamamoto M, Moritani M, Chang Z, Taki I, Tomita A, Ono T, Bae YC, Shigenaga Y, Yoshida A (2007) The somatotopic organization of trigeminal premotoneurons in the cat brainstem. Brain Res 1149:111-117.
Yamaoka A, Inoue T, Hironaka S, Nemoto A, Mukai Y, Itabashi K (2005) Postnatal changes in electrophysiological properties of rat jaw-closing motoneurons. Showa Univ J Med Sci 17:71-79.
Yasui Y, Itoh K, Mitani A, Takada M, Mizuno N (1985) Cerebral cortical projections to the reticular regions around the trigeminal motor nucleus in the cat. J Comp Neurol 241:348-356.
Yoshida A, Fukami H, Nagase Y, Appenteng K, Honma S, Zhang LF, Bae YC, Shigenaga Y (2001) Quantitative analysis of synaptic contacts made between functionally identified oralis neurons and trigeminal motoneurons in cats. J Neurosci 21:6298-6307.
Yoshida A, Taki I, Chang Z, Iida C, Haque T, Tomita A, Seki S, Yamamoto S, Masuda Y, Moritani M, Shigenaga Y (2009) Corticofugal projections to trigeminal motoneurons innervating antagonistic jaw muscles in rats as demonstrated by anterograde and retrograde tract tracing. J Comp Neurol 514:368-386.
Zhang GX, Sasamoto K (1990) Projections of two separate cortical areas for rhythmical jaw movements in the rat. Brain Res Bull 24:221-230.

実験 2)

背景

咀嚼運動は、下顎が上下に動いて歯牙で食物を噛み砕くだけでなく、舌や頬で食物を上下臼歯間に保持し、噛み砕いた食物が口腔外に漏出しないように口唇が閉鎖されるなど、さまざまな筋がそれぞれ正確なタイミングで動く、高度に協調した運動である。咀嚼のパターンジェネレーターは、顎口腔領域の感覚情報をもとに下顎、口唇、頬、舌の協調運動パターンを形成していると考えられるが、その詳細は明らかでない。

咀嚼のパターンジェネレーターによって形成された運動指令は、最終的にプレモーターニューロンによって、下顎、口唇、頬、舌の運動を遂行する各筋、すなわち開口筋、閉口筋、表情筋、舌筋の運動ニューロンに伝えられる。これまでの組織学的研究や電気生理学的研究の結果から、開口筋、閉口筋、表情筋、舌筋のプレモーターニューロンは、脳幹網様体や三叉神経感覚核を始め、脳幹の広い領域に互いに混じりあって存在することが知られている。したがって、開口筋、閉口筋、表情筋、舌筋のプレモーターニューロン群の一部が比較的近い部位に存在し、咀嚼のパターンジェネレーターからの指令を同時に受けることで協調して活動し、下顎、口唇、頬、舌の協調運動を実現している可能性がある。

そこで本研究は、まず開口筋・閉口筋と表情筋との協調機構に着目し、ラットの脳幹スライス標本に膜電位感受性色素を用いた光学的電位測定法を適用し、電気刺激によって開口筋・閉口筋の運動ニューロンが存在する三叉神経運動核と表情筋の運動ニューロン

が存在する顔面神経核に同時に興奮性の光学的応答を誘発する部位の検索を行った。さらに、開口筋あるいは閉口筋運動ニューロンと顔面神経運動ニューロンの同時パッチクランプ記録を行い、電気刺激あるいはレーザー光による caged グルタミン酸の解離による光刺激に対する応答様式を解析し、開口筋・閉口筋と表情筋との協調運動の神経機構を検討した。

実験方法

標本

Wistar 系ラット(P0-3)を用いて、三叉神経運動核(MoV)と顔面神経核(MoVII)を含む厚さ 400 ‐m の矢状断脳幹スライス標本を作成した。パッチクランプ記録を行う際は、スライス標本作成１－２日前に、cholera toxin subunit B Alexa Fluor® 488 conjugate (CTB, 0.5 mg/ml, 5 ‐l)を咬筋および周囲の表情筋に注入し、3,000 MW の dextran-tetramethylrhodamine-lysine (RDL, 10%, 2 ‐l)を顎二腹筋に注入し、閉口筋運動ニューロン(MMN)、開口筋運動ニューロン(DMN)、表情筋運動ニューロン(FMN)を逆行性に標識した。

人工脳脊髄液 (ACSF) の組成は以下の通りである。NaCl 130mM, KCl 3mM, NaH_2PO_4 1.25mM, $NaHCO_3$ 26mM, Glucose 10mM, $CaCl_2$ 2mM, $MgCl_2$ 2mM。光学的膜電位測定には、Di-4-ANNEPS (100 ‐g/ml)を用いてスライス標本を染色し、MICAM ULTIMA (Brain Vision)を用いて光学的応答を測定した。

ホールセルパッチクランプ記録は、Axopatch 700B amplifier (Molecular Devices)を用いて、RDL によって逆行性に標識された MMN および FMN の同時パッチクランプ記録あるいは DMN から単独のパッチクランプ記録を行った。記録電極内液(mM)は、次の 2 種類を用いた。1) -gluconate 130mM, KCl 27mM, $CaCl_2$ 1mM, HEPES 10mM, EGTA 11mM, $MgCl_2$ 2mM, NaGTP 0.3mM, NaATP 2mM, QX314 5mM (pH 7.3, 285-300 mOsm); 2) luconate 135mM, $CaCl_2$ 0.2mM, HEPES 10mM, EGTA 5mM, NaGTP 0.2mM, MgATP 2mM, QX314 5mM (pH 7.3, 285-300 mOsm)

光刺激

窒素パルスレーザー装置(波長 365 nm, パルス幅 600 ps; Micropoint, Photonic Instruments, Kawasaki, Japan)を用い、ガルバノミラーを介してレーザー光をスライス標本上の 5×5 の 25 点に照射し、あらかじめ灌流液中に投与した caged glutamate (4-methoxy-7-nitroindolinyl-caged L-glutamate, 300 ‐M, Tocris Cookson)の uncaging によりグルタミン酸を解離し、化学刺激を行った。レーザー光照射の制御ソフトウェアには、Metamorph (Molecular Devices)を用いた。

結果および考察

新生仔ラット矢状断脳幹スライス標本のさまざまな部位を電気刺激し、三叉神経運動核 (MoV) と顔面神経核 (MoⅦ) に光学的応答を誘発する部位を検索した。その結果、MoV と MoⅦの間の網様体 (rfV-Ⅶ) の電気刺激によって潜時 3ms で MoV と MoⅦの両方に光学的応答が誘発され、刺激後 6 ms (*) で最大となった. 両運動核の光学的応答は、CNQX と APV の同時投与、および strychnine と SR95531 の同時投与で減弱した (Fig.1)。さらに TTX を投与すると、応答は完全に消失した。すべての薬物を洗い流すと、20 分後に応答の回復が一部認められた。

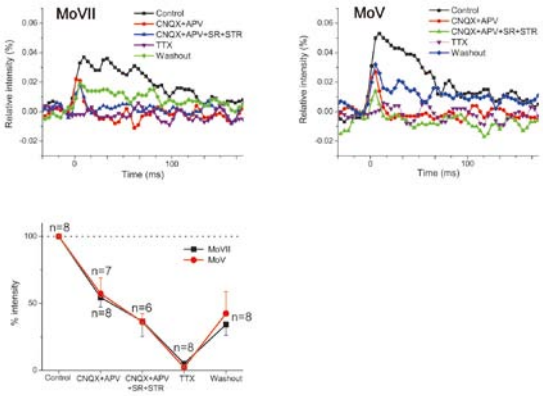

Fig.1　三叉神経運動核と顔面神経核との間の網様体 (rfV-Ⅶ) の電気刺激で、両運動核に光学的応答が同時に誘発される

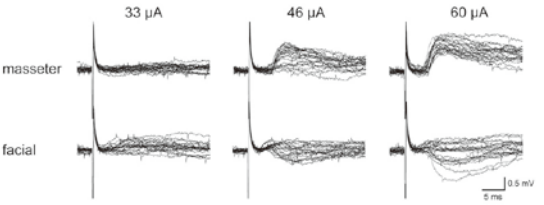

Fig.2　rfV-Ⅶの電気刺激で閉口筋運動ニューロンおよび顔面神経核運動ニューロンにシナプス後電位 (PSP) が同時に記録された

次に MoV と MoVII から同時パッチクランプ記録を行い、rfV-Ⅶ電気刺激によって誘発された咬筋運動ニューロンと顔面神経運動ニューロンのシナプス後電位 (PSP) を観察した. Figure 2 に代表的な例を示すが、この例では顔面神経運動ニューロンに誘発された PSP の閾値が 33 μA であったのに対して (下段左)、咬筋運動ニューロンの PSP の閾値は

46 μA であった（上段中）．刺激の強度を上げると、PSP の振幅が脱分極方向に増すものと、過分極性の PSP が現れるものがあった．記録した 5 組の運動ニューロンのペアーの全てで PSP の閾値はそれぞれ異っており、単一のプレモーターニューロンが咬筋運動ニューロンと表情筋運動ニューロンの両方に軸索を送ることを示す例は無かった．

さらに、MoV と MoVII から同時パッチクランプ記録を行い、rfV-Ⅶを 25 個の領域に分けてレーザー光を照射して caged glutamate を uncaging し、放出された微量なグルタミン酸によってプレモーターニューロンを刺激し、咬筋運動ニューロンおよび表情筋運動ニューロンに誘発されたシナプス後電流（PSC）を観察した．その結果、6、7、8、11 の領域の光刺激によって約 10-20ms の潜時で咬筋運動ニューロンに内向きの PSC が誘発された（Fig.3　上段）。特に、RdVII 領域である 6、11 の刺激で大きな PSC が観察された．一方、表情筋運動ニューロンでは、12、13、17、18 の刺激によって約 10-20ms の潜時で PSC が誘発された．この例では、咬筋運動ニューロンと顔面神経運動ニューロンに同時に PSC を誘発する刺激部位は認められなかった．

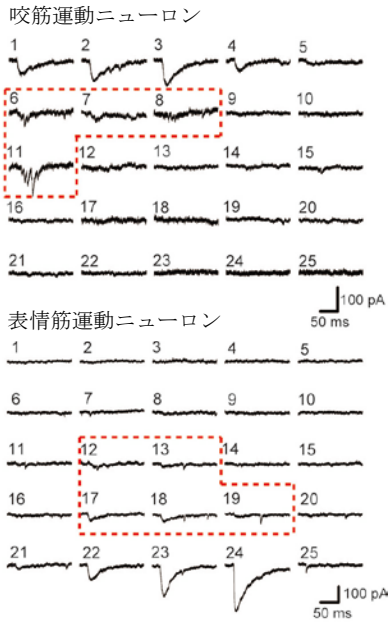

Fig.3　rfV-Ⅶの光刺激で咬筋運動ニューロンと表情筋運動ニューロンにシナプス後電流（PSC）が誘発された

以上の結果から、閉口筋運動ニューロンに対するプレモーターニューロンと表情筋運動ニューロンに出力を送るプレモーターニューロン群は rfV-Ⅶに存在するが、両プレモーターニューロンの存在部位は重ならない可能性がある。したがって、各筋のプレモーターニューロンはその存在部位によって性質が異なり、下顎と頬、口唇などの協調運動の制御は、プレモーターニューロンより上位の神経回路で行われる可能性が考えられる。

５．主な発表論文等
（研究代表者、研究分担者及び連携研究者には下線）

〔雑誌論文〕（計１４件）

① Liu L, Tsuruoka M, Maeda M, Hayashi B, Wang X, Inoue T.　Descending modulation of visceral nociceptive transmission from the locus coeruleus/subcoeruleus in the rat. Brain Res Bull. 76(6):616-25, 2008 Aug.

② Nakamura S, Inoue T, Nakajima K, Moritani M, Nakayama K, Tokita T, Yoshida A and Maki K　Synaptic transmission from the supratrigeminal region to jaw-closing and jaw-opening motoneurons in developing Rats. J. Neurophysiol. 100: 1885-1896, 2008 October.

③ Maeda M, Tsuruoka M, Hayashi B, Nagasawa I, Inoue T.　Descending pathways from activated locus coeruleus/subcoeruleus following unilateral hindpaw inflammation in the rat. Brain Res Bull., 78: 170-174, 2009 Mar 16.

④ Tokita K, Inoue T and Boughter Jr J.D. Afferent connections of the parabrachial nucleus in C57BL/6J mice. Neuroscience, 161: 475-488, 2009 Jun 30.

⑤ Takami M, Mochizuki A, Yamada A, Tachi K, Zhao B, Miyamoto Y, Anada T, Honda Y, Inoue T, Nakamura M, Suzuki O, Kamijo R. Osteoclast differentiation induced by synthetic octacalcium phosphate through RANKL expression in osteoblasts. Tissue Eng Part A, 15: 3991-4000, 2009 Jul 13.

⑥ Tsuruoka M, Wang D, Tamaki J, Inoue T. Descending influence from the nucleus locus coeruleus/subcoeruleus on visceral nociceptive transmission in the rat spinal cord. Neuroscience, 165 : 1019-1024, 2010 Feb 17.

⑦ Gemba-Nishimura A, Inoue T, Nakamura S, Nakayama K, Mochizuki A, Shintani S and Yoshimura S　Properties of synaptic transmission from the reticular formation dorsal to the facial nucleus to trigeminal motoneurons during early postnatal development in rats. Neuroscience, 166 :　1008-1022, 2010 Mar 31.

⑧ Tsuruoka M, Tamaki J Maeda M, Hayashi B and Inoue T. The nucleus locus coeruleus/subcoeruleus affects the defensive-like, immobile posture following an air-puff startle reaction in the rat. Neuroscience, 168: 149-155, 2010 Jun 16.
⑨ Haino T, Hironaka S, Ooka T, Tokita K, Kubota Y, Boughter Jr JD, Inoue T and Mukai Y. Orosensory deprivation alters taste-elicited c-Fos expression in the parabrachial nucleus of neonatal rats. Neurosci Res, 67: 228-235, 2010, July.
⑩ Wang X, Suzawa T, Ohtsuka H, Zhao B, Miyamoto Y, Miyauchi T, Nishimura R, Inoue T, Nakamura M, Baba K, Kamijo R. Carbonic anhydrase II regulates differentiation of ameloblasts via Intracellular pH-dependent JNK signaling pathway. J Cell Physiol, 225: 709-719, 2010, November.
⑪ Tokita K, Inoue T and Boughter Jr J.D. Subnuclear organization of parabrachial efferents to the thalamus, amygdala and lateral hypothalamus in C57BL/6J mice: a quantitative retrograde double labeling study. Neuroscience, 171(1): 351-65, 2010, Nov 24.
⑫ Tachi K, Takami M, Zhao B, Mochizuki A, Yamada A, Miyamoto Y, Inoue T, Baba K, Kamijo R. Bone morphogenetic protein 2 enhances mouse osteoclast differentiation via increased levels of receptor activator of NF-κB ligand expression in osteoblasts. Cell and Tissue Research, 342(2):213-20, 2010 Nov.
⑬ Tachi K, Takami M, Sato H, Mochizuki A, Zhao B, Miyamoto Y, Tsukasaki H, Inoue T, Shintani S, Koike T, Honda Y, Suzuki O, Baba K, Kamijo R. Enhancement of bone morphogenetic protein-2-induced ectopic bone formation by transforming growth factor β1. Tissue Eng Part A. 17(5-6): 597-606, 2011 March.
⑭ Matsuo E, Mochizuki A, Nakayama K, Nakamura S, Yamamoto T, Shioda S, Sakurai T, Yanagisawa M, Shiuchi T, Minokoshi Y, Inoue T. Decreased intake of sucrose solutions in orexin knockout mice. J Mol Neurosci, 43(2): 217-24, 2011 Feb.

〔学会発表〕(計３２件)
① Nakayama K, Ihara Y, Inoue T. Rhythmic motor activity evoked by electrical stimulation of the trigeminal nerve sensory root in neonatal mice. 第 88 回日本生理学会 第 116 回日本解剖学会総会・全国学術集会合同大会, 横浜, 2011/3/28
② Ihara Y, Nakayama K, Takahashi K, Inoue T. Left and right coordination of NMDA-induced rhythmic activities in the trigeminal nerves of neonatal mice in vitro. 第 88 回日本生理学会 第 116 回日本解剖学会総会・全国学術集会合同大会, 横浜, 2011/3/28
③ Matsuo E, Mochizuki A, Nakayama K, Nakamura S, Yamamoto T, Shioda S, Sakurai T, Inoue T. Decreased sucrose intake and locomotor activity in orexin knockout mice. The 89th General Session & Exhibition of the International Association for Dental Research Meeting Location, San Diego 2011/3/19
④ Nakamura S, Bradley RM. Characteristics of calcium and sodium currents in rat geniculate ganglion neurons. Society for Neuroscience 40th annual meeting, San Diego 2010/11/17
⑤ Nakayama K, Ihara Y, Inoue T. Neuronal mechanisms generating electrical stimulation-evoked rhythmic burst activity in the trigeminal nerve of neonatal mice. Society for Neuroscience 40th annual meeting, San Diego 2010/11/15
⑥ 中山希世美、望月文子、西村晶子、井上富雄 新生マウス 脳幹摘出標本におけるリズミックな顎運動の誘発, 日本顎口腔機能学会 第４５回学術大会, 埼玉, 2010/11/6
⑦ 中山希世美、伊原良明、井上富雄, 新生マウス脳幹摘出標本における三叉神経刺激誘発リズムに関与する神経伝達物質, 第 33 回日本神経科学大会, 神戸, 2010/9/2
⑧ 玉置潤一郎、鶴岡正吉、前田昌子、林文祥、井上富雄, ラット驚愕反応に伴う痛み抑制. 第 33 回日本神経科学大会, 神戸, 2010/9/2
⑨ 玉置潤一郎、鶴岡正吉、王丹、前田昌子、林文祥、井上富雄, 内臓痛と内臓―体性反射に対する青斑核刺激効果の解離, 第 87 回日本生理学会, 岩手, 2010/5/21
⑩ 中山希世美、望月文子、井上富雄, 三叉神経中脳路核ニューロンにおけるオレキシンの作用, 第 7 回 GPCR 研究会, 東京, 2010/5/11
⑪ Matsuo E, Mochizuki A, Nakayama K, Inoue T. Decreased intake of sucrose solutions in orexin knockout mice. GPCR2010 Symposium, Kyoto, 2010/3/30
⑫ 舘慶太、高見正道、佐藤華、本田義知、宮

本阿礼、望月文子、井上富雄、新谷悟、中村雅典、鈴木治、馬場一美、上條竜太郎, TGF-βはBMP2に誘導された異所性骨形成を促進する, 第 32 回日本分子生物学会, 横浜, 2009/12/9-12

⑬ 望月文子、中山希世美、中村史朗、井上富雄. 三叉神経中脳路核ニューロンに対するオレキシンの作用, 第46回日本口腔組織培養学会学術大会, 東京, 2009/12/5

⑭ 舘慶太、高見正道、佐藤華、本田義知、望月文子、井上富雄、新谷悟、中村雅典、鈴木治、上條竜太郎、馬場一美, TGF-β1はBMP-2 による異所性骨形成を強力に促進する, 第 2 回再生補綴医学研究会, 名古屋, 2009/11/27

⑮ Inoue T, Nakayama K, Mochizuki A, Nakamura S, Shioda S. Effects of orexin on activities of mesencephalic trigeminal sensory neurons in developing rats. Society for Neuroscience 39th annual meeting, Chicago 2009/10/17

⑯ Nakamura S, Bradley R.M. Calcium conductance of neurons in the rat geniculate ganglion innervating the anterior tongue. Society for Neuroscience 39th annual meeting, Chicago 2009/10/17

⑰ 玉置潤一郎、鶴岡正吉、前田昌子、林文祥、井上富雄, 青斑核は驚愕反応に伴う不動期に関与する, 第32回日本神経科学大会, 名古屋, 2009/9/17

⑱ 中山希世美、伊原良明、井上富雄, 新生マウス脳幹摘出標本における三叉神経刺激による顎運動の誘発, 第32回日本神経科学大会, 名古屋, 2009/9/17

⑲ 井上富雄、望月文子、中山希世美, オレキシンの三叉神経中脳路核ニューロン活動に対する影響, 第51回歯科基礎医学会学術大会, 新潟, 2009/9/11

⑳ 中山希世美、伊原良明、井上富雄, 新生マウス脳幹摘出標本において三叉神経の電気刺激により誘発される顎運動, 第51回歯科基礎医学会学術大会, 新潟, 2009/9/11

21 Tsuruoka M, Wang D, Tamaki J, Maeda M, Hayashi B, Inoue T. Characterization of coeruleospinal modulation on visceral pain processing in the rat spinal cord. 第86回日本生理学会大会, 京都, 2009/7/27-8/1

22 舘慶太、高見正道、佐藤華、本田義知、宮本阿礼、望月文子、井上富雄、新谷悟、中村雅典、鈴木治、馬場一美、上條竜太郎, TGF-βは BMP-2 による異所性骨形成を協力に促進する, 第27回日本骨代謝学会学術大会, 大阪, 2009/7/23-25

23 舘慶太、高見正道、馬場一美、山田篤、望月文子、井上富雄、上條竜太郎, BMP-2とヘパリンによる破骨細胞分化の作用, 第31回日本分子生物学会学術大会, 神戸, 2008/12

24 Nakamura S, Moritani A, Yoshida A, Inoue T. Properties of synaptic transmission from the supratrigeminal region to the trigeminal motoneurons in developing rats. Society for Neuroscience's 38th annual meeting, Washington DC 2008/11/18

25 Gemba A, Nakamura S, Tsuruoka M, Yoshimura S, Inoue T. Synaptic transmission from the reticular formation dorsal to the facial nucleus to jaw-closing motoneurons in developing rats. Society for Neuroscience's 38th annual meeting, Washington DC 2008/11/15

26 舘慶太、高見正道、馬場一美、山田篤、望月文子、井上富雄、上條竜太郎, BMP-2とTGF-▪による破骨細胞分化調節, 第45回日本口腔組織培養学会学術大会, 松本, 2008/11

27 舘慶太、高見正道、馬場一美、山田篤、望月文子、井上富雄、上條竜太郎, ヘパリンと BMP-2 は骨芽細胞を介して相乗的に破骨細胞分化を促進する, 第26回日本骨代謝学会学術大会, 大阪, 2008/10

28 前田昌子、林文祥、中村史朗、中山希世美、望月文子、松尾英子、鶴岡正吉、井上富雄, 味覚の情報伝達は内臓痛によって抑制される, 第21回日本歯科医学会総会, 横浜, 2008/10/15

29 玄番晶子、中村史朗、望月文子、井上富雄, ラットにおける顔面神経核背側網様体から三叉神経運動ニューロンへのシナプス入力, 第 50 回歯科基礎医学会学術大会, 東京, 2008/9/23

30 前田昌子、林文祥、鶴岡正吉、井上富雄, 延髄孤束核における味覚性 c-fos 発現は内臓侵害刺激によって抑制される, 第50回歯科基礎医学会学術大会, 東京, 2008/9/23

31 舘慶太、高見正道、馬場一美、山田篤、望月文子、井上富雄、上條竜太郎, ヘパリンと BMP-2 は骨芽細胞を介して破骨細胞分化を促進する, 第50回歯科基礎医学会学術大会, 東京, 2008/9/23

32 Nakayama K, Mochizuki A, Nakamura S, Inoue T. Orexin modulates neuronal activities of mesencephalic trigeminal sensory neurons in rats. Showa University International Symposium for Life Science 5th Annual Meeting, Tokyo, 2008/9/2

〔図書〕（計８件）

① 増田裕次、井上富雄, 顎口腔系の機能評価のための生理学;顎口腔機能の評価, 鳴門市, 2010, 日本顎口腔機能学会, pp59－65
② Kamijo R, Zhao B, Mochizuki A, Inoue T, Takami M, Involvement of transcription factor IRF-8 in bone metastasis of cancer. Tokyo, 2010, The Waksman Foundation of Japan
③ 井上富雄, 咬合と咀嚼･吸啜 ④摂食行動、⑤咀嚼能力、⑥吸啜； 最新衛生士教本 歯・口腔の構造と機能 口腔解剖学・口腔組織発生学･口腔生理学. 全国歯科衛生士教育協議会 監修；前田健康、遠藤圭子、畠山能子編, 東京, 2011, 医歯薬出版,pp96-104
④ 井上富雄（分担執筆）, 生理学的にみた歯周組織；ザ・ペリオドントロジー, 和泉雄一、沼部幸博、山本松男、木下淳博 編, 東京, 2009, 永末出版, pp32-35
⑤ 井上富雄, 日本歯科医学会学術用語集, 日本歯科医学会編, 東京, 2008, 医歯薬出版
⑥ 井上富雄, 筋電図･顎運動の基礎－運動単位と筋の張力－, 顎運動および筋電図検査法,鳴門市, 2008, 日本顎口腔機能学会, pp35-38
⑦ 井上富雄, 系統的な科学的推論を用いた顎口腔機能研究法, 顎運動および筋電図法, 鳴門市, 2008, 日本顎口腔機能学会, pp54-59
⑧ Nakayama K, Mochizuki A, Nakamura S, Inoue T. Orexin modulates neuronal activities of mesencephalic trigeminal sensory neurons in rats. Tansmitters and Modulators in Health and Disease. I. Homma, S. Shioda, N. Kato (Eds), Tokyo, 2009, Springer, pp179-182

〔産業財産権〕
○出願状況（計０件）
○取得状況（計０件）

〔その他〕
ホームページ等
http://www.showa-u.ac.jp/sch/dent/major/oralphys/index.html

６．研究組織
(1)研究代表者
井上　富雄（INOUE TOMIO）
昭和大学歯学部口腔生理学教室・教授
研究者番号：70184760

(2)研究分担者
中村　史朗（NAKAMURA SHIRO）
昭和大学歯学部口腔生理学教室・助教
研究者番号：60384187
中山　希世美（NAKAYAMA KIYOMI）
昭和大学歯学部口腔生理学教室・助教
研究者番号：00433798
望月　文子（MOCHIZUKI AYAKO）
昭和大学歯学部口腔生理学教室・助教
研究者番号：10453648

(3)連携研究者
なし